



the
abdus salam
international centre for theoretical physics

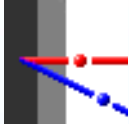
H4.SMR/1503 - 12

**WORKSHOP ON NUCLEAR DATA FOR SCIENCE AND
TECHNOLOGY: MATERIALS ANALYSIS**

(19 - 30 May 2003)

RBS - Rutherford Backscattering Spectrometry

Dr. Matej Mayer
Max-Planck-Institut Fuer Palsmaphysik
EURATOM Association
Garching
GERMANY

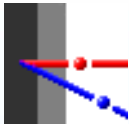


RBS - Rutherford Backscattering Spectrometry

M. Mayer

Max-Planck-Institut für Plasmaphysik, EURATOM Association, 85748 Garching, Germany

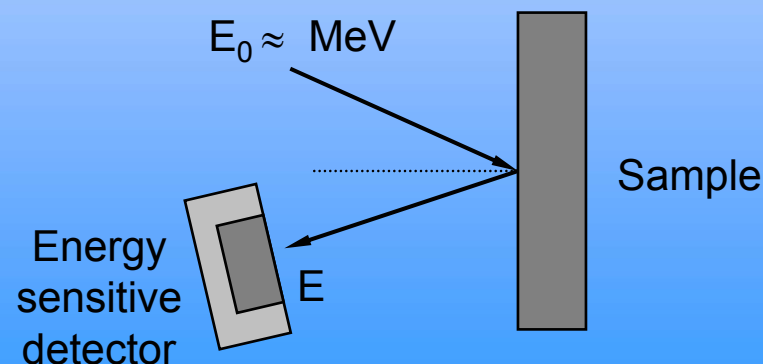
- History
- Scattering geometry and kinematics
- Rutherford cross section and limitations
- RBS spectra from thin and thick films
- Stopping power and energy loss
- Detector resolution
- Energy loss straggling
- Cross sections from selected light elements
 - incident ^1H
 - incident ^4He

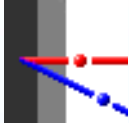


Introduction

RBS - Rutherford Backscattering Spectrometry

- Widely used for near-surface layer analysis of solids
- Elemental composition and depth profiling of individual elements
- Quantitative without reference samples (\neq SIMS, sputter-XPS,...)
- Non-destructive (\neq SIMS, sputter-XPS,...)
- Analysed depth: 2 μm (He-ions); 20 μm (protons)
- Very sensitive for heavy elements: \approx ppm
- Less sensitive for light elements \Rightarrow NRA

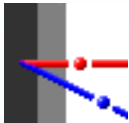




Introduction (2)

Rutherford Backscattering (RBS) is

- **Elastic** scattering of protons, ${}^4\text{He}$, ${}^{6,7}\text{Li}$, ...
 - ≠ Nuclear Reaction Analysis (NRA): Inelastic scattering, nuclear reactions
 - ≠ Detection of recoils: Elastic Recoil Detection Analysis (ERD)
 - ≠ Particle Induced X-ray Emission (PIXE)
 - ≠ Particle Induced γ -ray Emission (PIGE)
- **RBS is a badly selected name, as it includes:**
 - Scattering with non-Rutherford cross sections
 - Back- and forward scattering
- Sometimes called **Particle Elastic scattering Spectrometry (PES)**
- Ion beam Analysis (IBA) acronyms: G. Amsel, Nucl. Instr. Meth. B118 (1996) 52

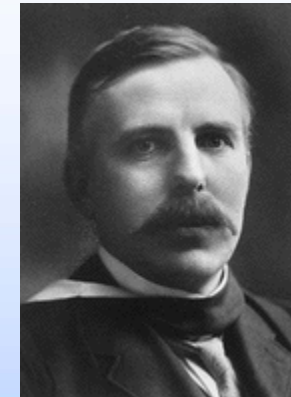


History



Sir Ernest Rutherford (1871 - 1937)

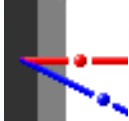
- 1911: Rutherford's scattering experiments: ${}^4\text{He}$ on Au
⇒ Atomic nucleus, nature of the atom



RBS as materials analysis method

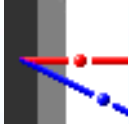
- 1957: S. Rubin, T.O. Passell, E. Bailey, "Chemical Analysis of Surfaces by Nuclear Methods", *Analytical Chemistry* 29 (1957) 736

"Nuclear scattering and nuclear reactions induced by high energy protons and deuterons have been applied to the analysis of solid surfaces. The theory of the scattering method, and determination of O, Al, Si, S, Ca, Fe, Cu, Ag, Ba, and Pb by scattering method are described. C, N, O, F, and Na were also determined by nuclear reactions other than scattering. The methods are applicable to the detection of all elements to a depth of several μm , with sensitivities in the range of 10^{-8} to 10^{-6} g/cm^2 ."



History (2)

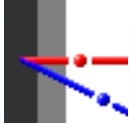
- 1970's: RBS becomes a popular method due to invention of silicon solid state detectors
- 1977: H.H. Andersen and J.F. Ziegler
Stopping Powers of H, He in All Elements
- 1977: J.W. Mayer and E. Rimini
Ion Beam Handbook for Materials Analysis
- 1979: R.A. Jarjis
Nuclear Cross Section Data for Surface Analysis
- 1985: M. Thompson
Computer code RUMP for analysis of RBS spectra
- 1995: J.R. Tesmer and M. Nastasi
Handbook of Modern Ion Beam Materials Analysis
- 1997: M. Mayer
Computer code SIMNRA for analysis of RBS, NRA spectra



Index

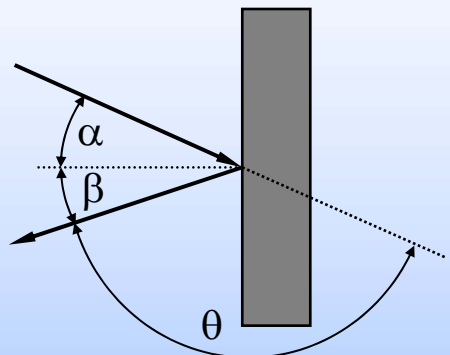
IPP

- History
- **Scattering geometry and kinematics**
- Rutherford cross section and limitations
- RBS spectra from thin and thick films
- Stopping power and energy loss
- Detector resolution
- Energy loss straggling
- Cross sections from selected light elements
 - incident ^1H
 - incident ^4He



Scattering Geometry

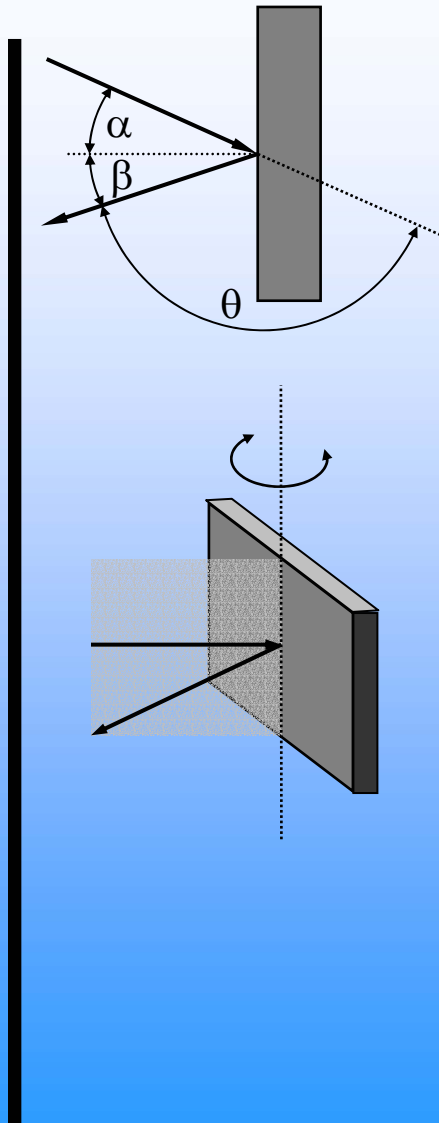
IPP



α : incident angle
 β : exit angle
 θ : scattering angle

Often (but not exclusive): $160^\circ \leq \theta \leq 170^\circ$

\Rightarrow optimised mass resolution



IBM geometry

Incident beam, exit beam, surface normal in one plane
 $\Rightarrow \alpha + \beta + \theta = 180^\circ$

Advantage: Simple

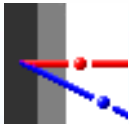
Cornell geometry

Incident beam, exit beam, rotation axis in one plane
 $\Rightarrow \cos(\beta) = -\cos(\alpha) \cos(\theta)$

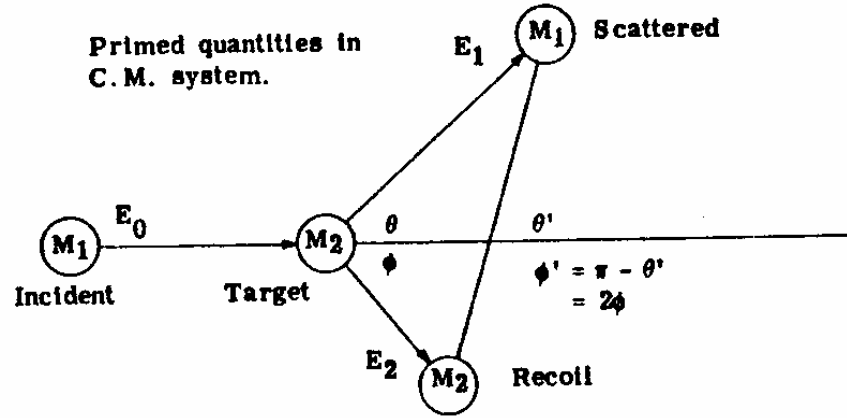
Advantage:
large scattering angle and grazing incident + exit angles
good mass and depth resolution simultaneously

General geometry

α, β, θ not related



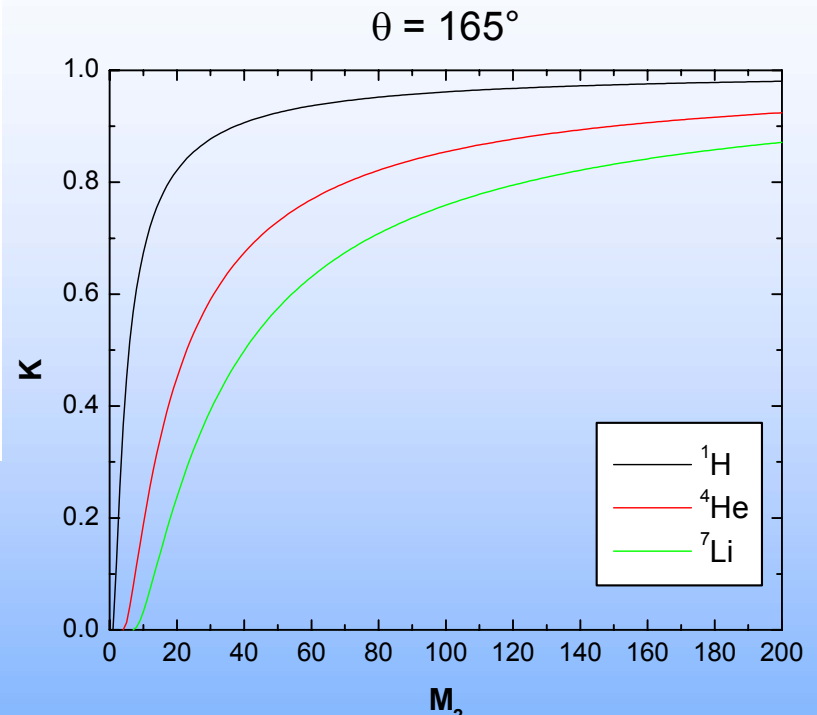
Scattering Kinematics



Elastic scattering: $E_0 = E_1 + E_2$

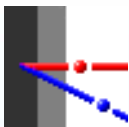
Kinematic factor: $E_1 = K E_0$

$$K = \left[\frac{(M_2^2 - M_1^2 \sin^2 \theta)^{1/2} + M_1 \cos \theta}{M_1 + M_2} \right]^2$$



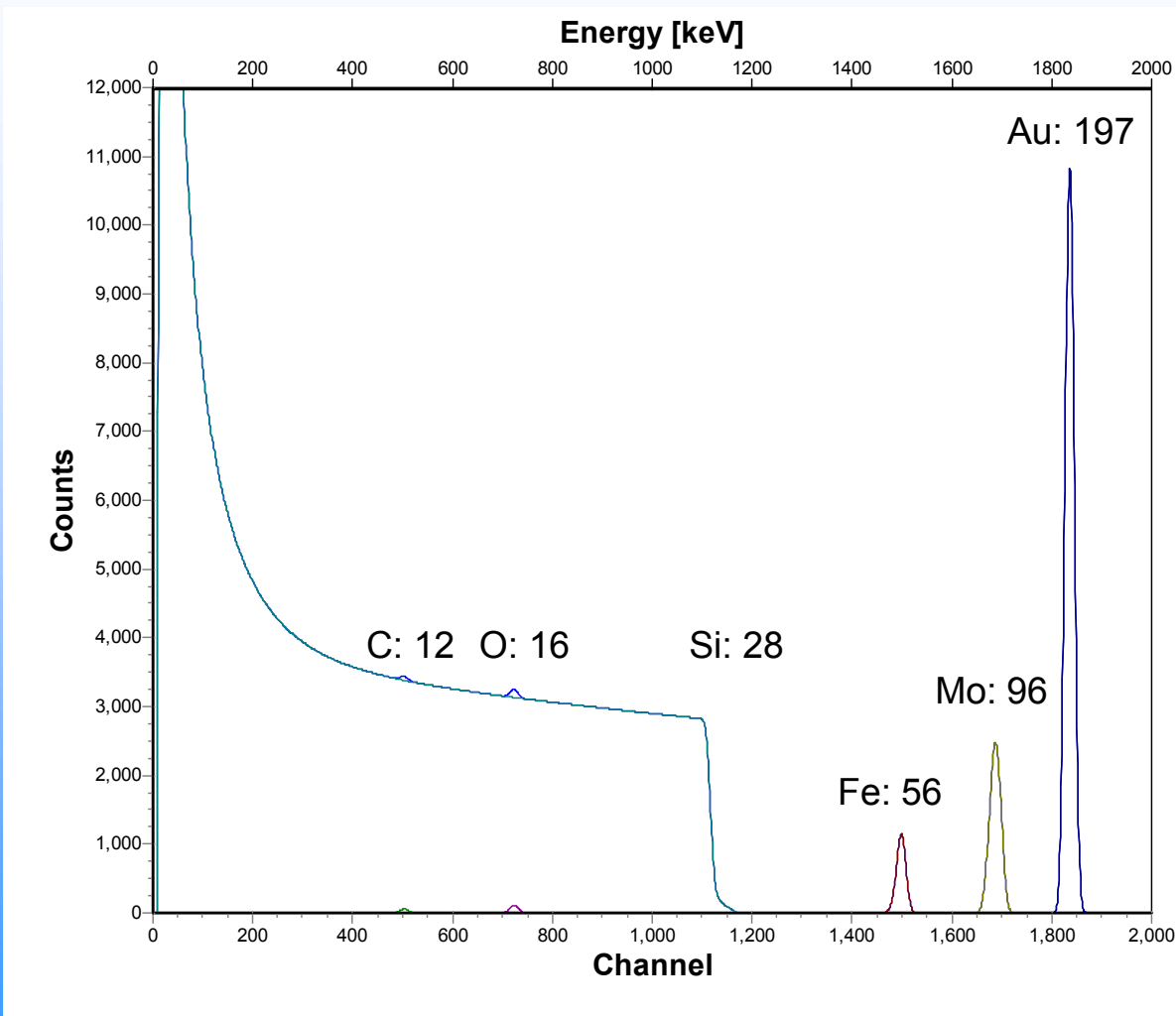
$$\Delta E_1 = E_0 \frac{dK}{dM_2} \Delta M_2$$

ΔE_1 : Energy separation
 ΔM_2 : Mass difference



Scattering Kinematics: Example (1)

IPP



2000 keV ${}^4\text{He}$, $\theta = 165^\circ$

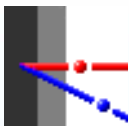
backscattered from

C, O, Fe, Mo, Au

3×10^{16} Atoms/cm² each

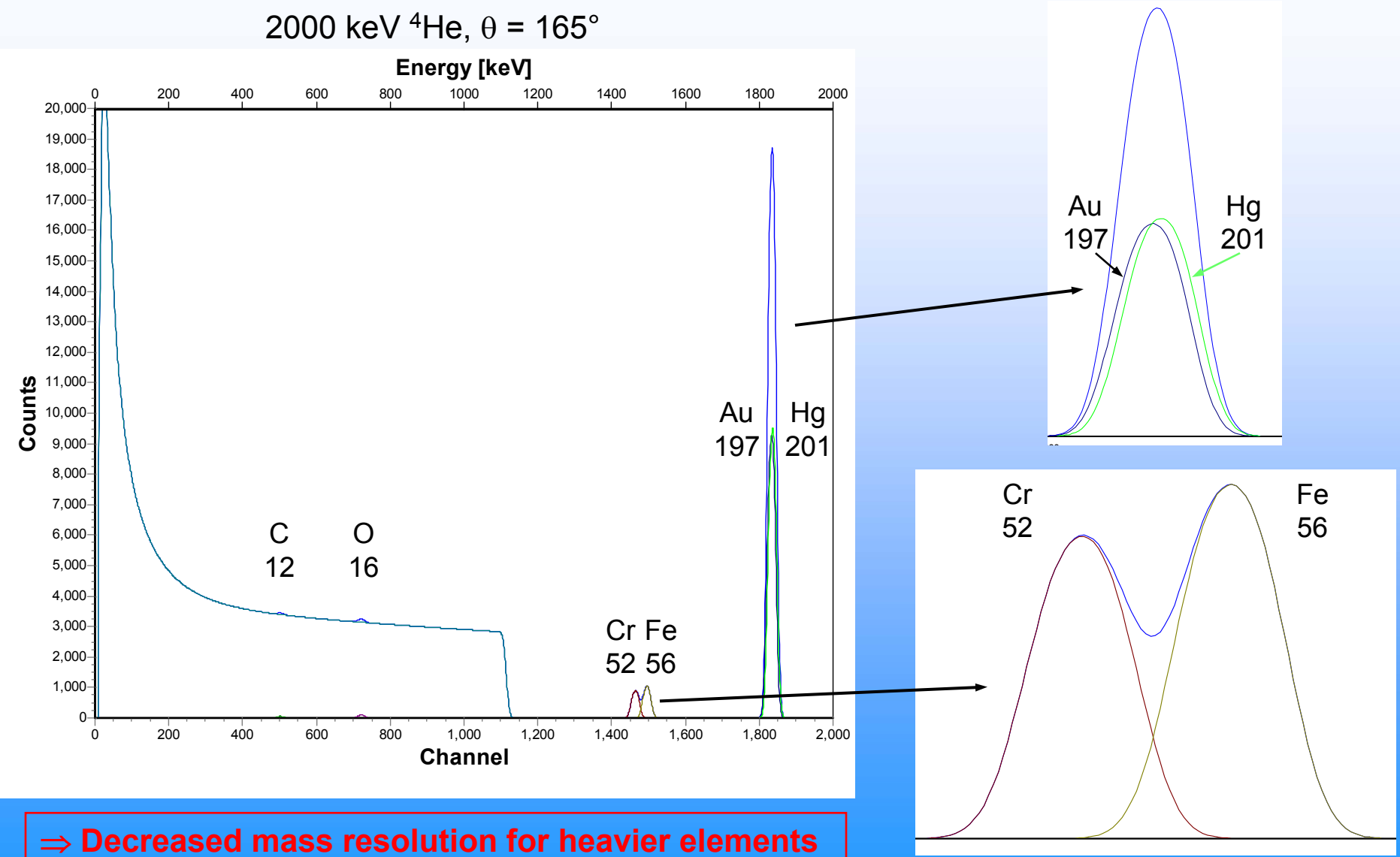
on Si substrate

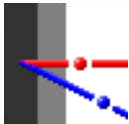
⇒ light elements may overlap
with thick layers of heavier
elements



Scattering Kinematics: Example (2)

IPP

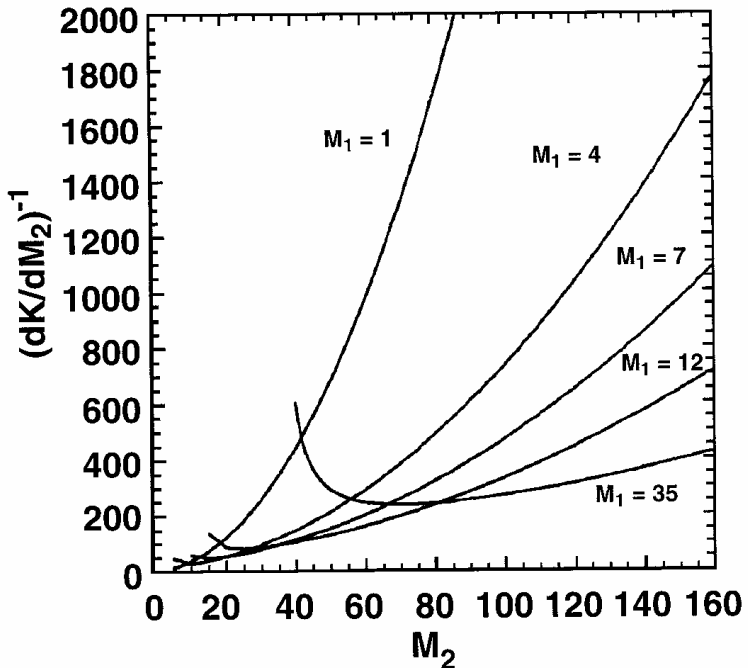




Mass Resolution

$$\Delta E_1 = E_0 \frac{dK}{dM_2} \Delta M_2 \quad \Rightarrow \quad \delta M_2 = \frac{\delta E}{E_0} \left(\frac{dK}{dM_2} \right)^{-1}$$

δM_2 : Resolvable mass difference
 δE : Energy resolution of the system



J.R. Tesmer and M. Nastasi,
Handbook of Modern Ion Beam Materials Analysis,
MRS, 1995

⇒ Improved mass resolution
with increasing M_1

But: For surface barrier detectors

$$\delta E = \delta E(M_1)$$

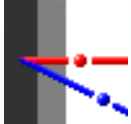
$\delta E(1)$: 12 keV

$\delta E(4)$: 15 keV

$\delta E(12)$: 50 keV

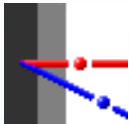
⇒ optimum mass resolution
for $M_1 = 4 - 7$

Heavier M_1 only useful with magnetic analysers,
time-of-flight detectors



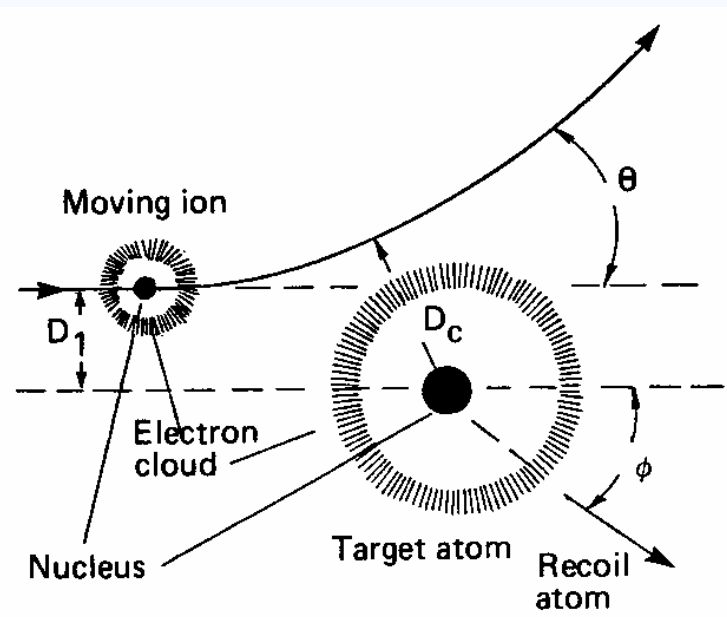
Index

- History
- Scattering geometry and kinematics
- **Rutherford cross section and limitations**
- RBS spectra from thin and thick films
- Stopping power and energy loss
- Detector resolution
- Energy loss straggling
- Cross sections from selected light elements
 - incident ^1H
 - incident ^4He



Rutherford Cross Section

IPP

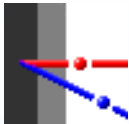


- Neglect shielding by electron clouds
- Distance of closest approach large enough that nuclear force is negligible
⇒ Rutherford scattering cross section

$$\sigma_R(E, \theta) = \left(\frac{Z_1 Z_2 e^2}{4E} \right)^2 \times \frac{4 \left[(M_2^2 - M_1^2 \sin^2 \theta)^{1/2} + M_2 \cos \theta \right]^2}{M_2 \sin^4 \theta (M_2^2 - M_1^2 \sin^2 \theta)^{1/2}}$$

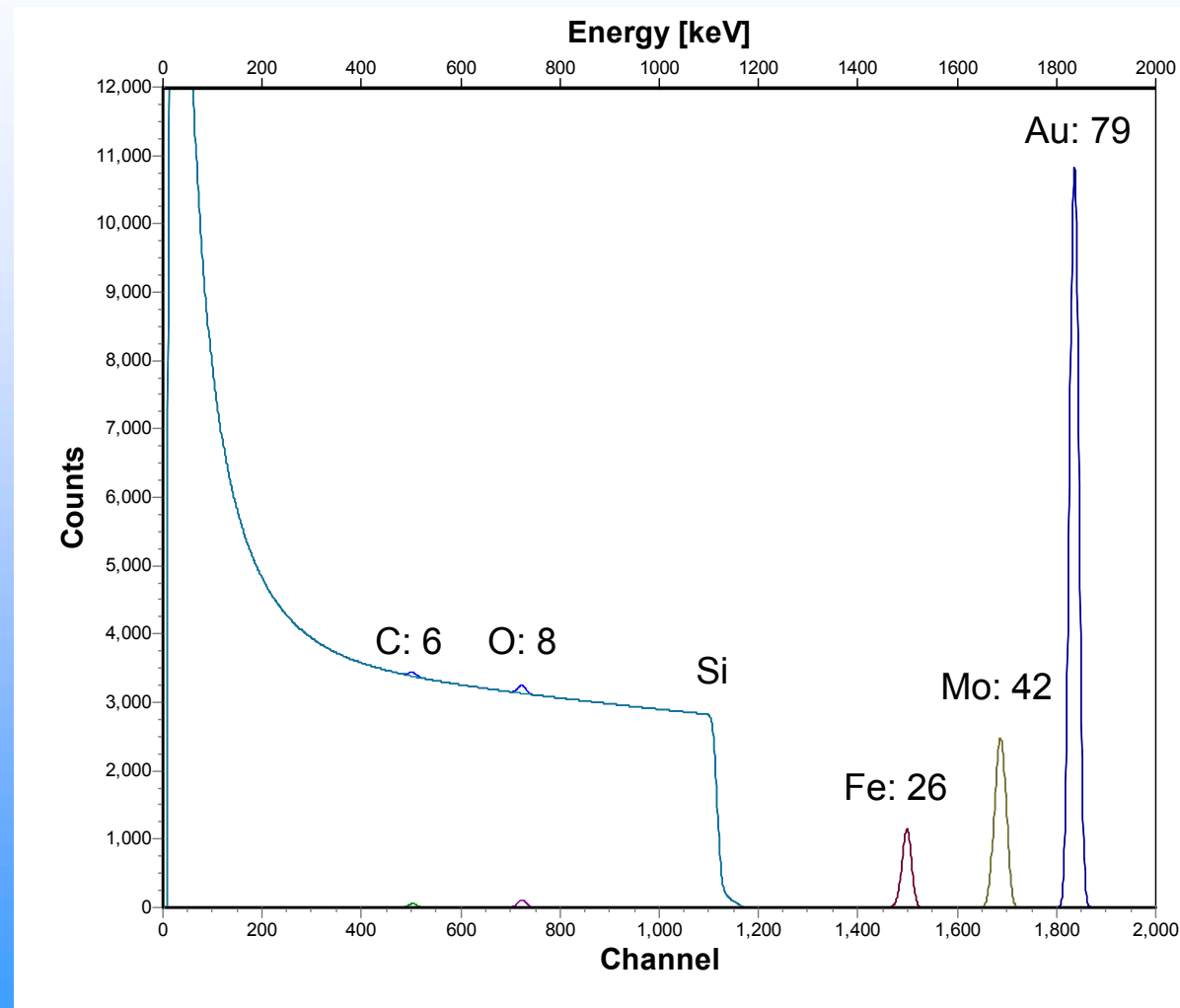
Note that: $\sigma_R \propto \frac{Z_1^2 Z_2^2}{E^2}$

- Sensitivity increases with
- increasing Z_1
 - increasing Z_2
 - decreasing E



Rutherford Cross Section: Example

IPP



2000 keV ${}^4\text{He}$, $\theta = 165^\circ$

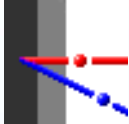
backscattered from

C, O, Fe, Mo, Au

3×10^{16} Atoms/cm² each

on Si substrate

- ⇒ Increased sensitivity for heavier elements $\propto Z_2^2$
- ⇒ Good for heavier elements on lighter substrate
- ⇒ Less good for lighter elements on heavier substrate



Shielded Rutherford Cross Section



Shielding by electron clouds gets important at

- low energies
- low scattering angles
- high Z_2

Shielding is taken into account by a shielding factor $F(E, \theta)$

$$\sigma(E, \theta) = F(E, \theta) \sigma_R(E, \theta)$$

$F(E, \theta)$ close to unity

$F(E, \theta)$ is obtained by solving the scattering equations
for a shielded interatomic potential:

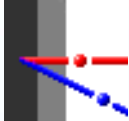
$$V(r) = \frac{Z_1 Z_2 e^2}{r} \varphi(r/a)$$

φ : Screening function

Use Thomas-Fermi or Lenz-Jenssen screening function

$$a: \text{Screening radius} \quad a = 0.885 a_0 (Z_1^{2/3} + Z_2^{2/3})^{-1/2}$$

a_0 : Bohr radius



Shielded Rutherford Cross Section (2)

For $90^\circ \leq \theta \leq 180^\circ$:

L'Ecuyer et al. (1979)

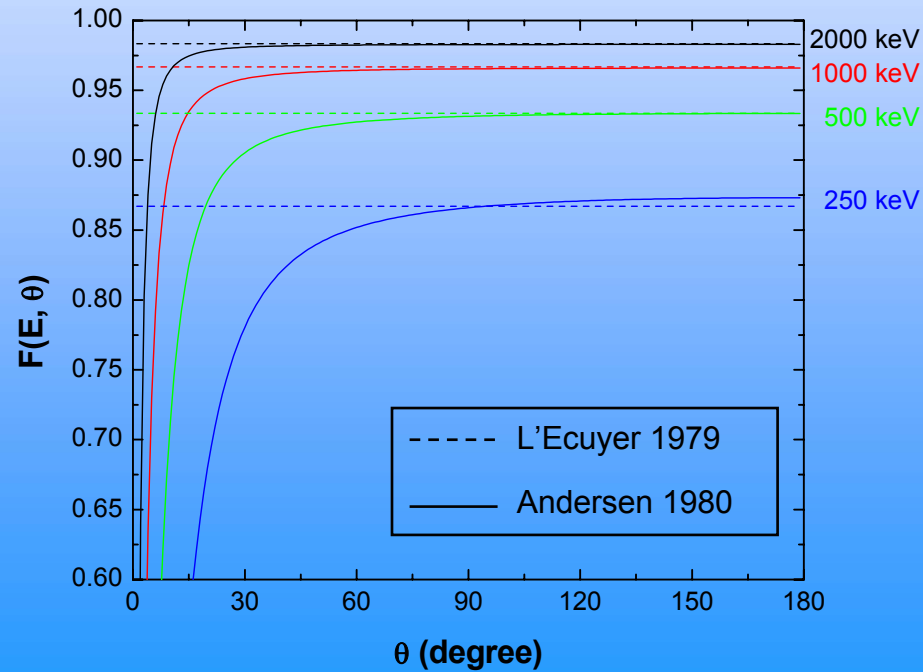
$$\frac{\sigma}{\sigma_R} = 1 - \frac{0.049 Z_1 Z_2^{4/3}}{E_{CM}}$$

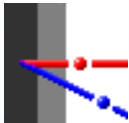
Wenzel and Whaling (1952)

$$\frac{\sigma}{\sigma_R} = 1 - \frac{0.0326 Z_1 Z_2^{7/2}}{E_{CM}}$$

For all θ : Andersen et al. (1980)

${}^4\text{He}$ backscattered from Au





Non-Rutherford Cross Section

Cross section becomes non-Rutherford if nuclear forces get important

- high energies
- high scattering angles
- low Z_2

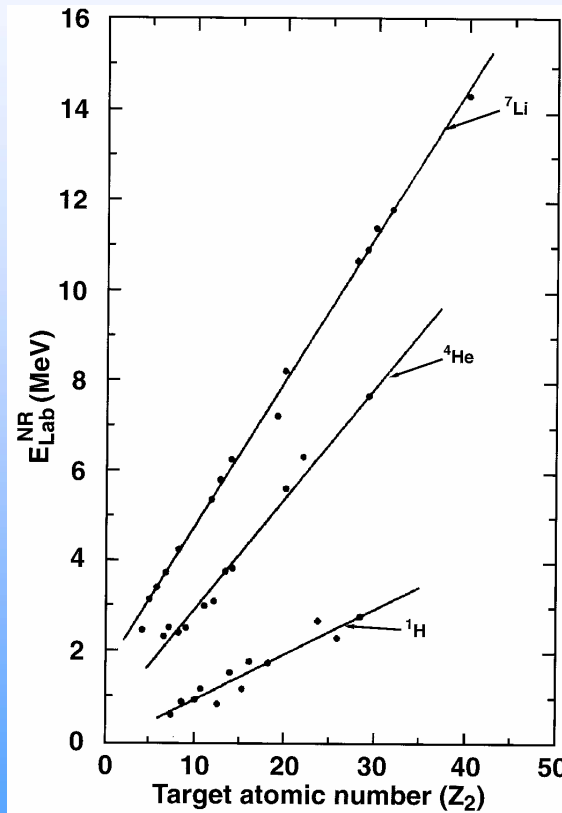
Energy at which the cross section deviates
by $> 4\%$ from Rutherford at $160^\circ \leq \theta \leq 180^\circ$
Bozoian (1991)

$${}^1\text{H}: E_{\text{Lab}}^{\text{NR}} = 0.12 Z_2 - 0.5 \quad [\text{MeV}]$$

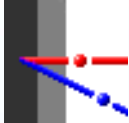
$${}^4\text{He}: E_{\text{Lab}}^{\text{NR}} = 0.25 Z_2 + 0.4 \quad [\text{MeV}]$$

Linear Fit to experimental values (${}^1\text{H}$, ${}^4\text{He}$)
or optical model calculations (${}^7\text{Li}$)

Accurate within ± 0.5 MeV

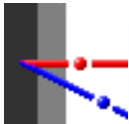


J.R. Tesmer and M. Nastasi,
Handbook of Modern Ion Beam Materials Analysis,
MRS, 1995



Index

- History
- Scattering geometry and kinematics
- Rutherford cross section and limitations
- **RBS spectra from thin and thick films**
- Stopping power and energy loss
- Detector resolution
- Energy loss straggling
- Cross sections from selected light elements
 - incident ^1H
 - incident ^4He



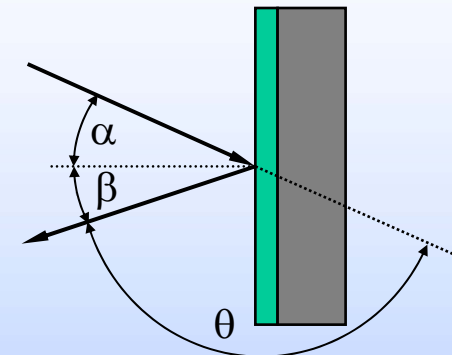
RBS-Spectrum of a thin layer

A layer is thin, if:

- Energy loss in layer < experimental energy resolution
- Negligible change of cross section in the layer

Energy E of backscattered particles:

$$E = K E_0$$



Number Q of backscattered particles:

$$Q = N_0 \Omega \sigma(E) \frac{\Delta x}{\cos \alpha}$$

Q : Number of counts in detector

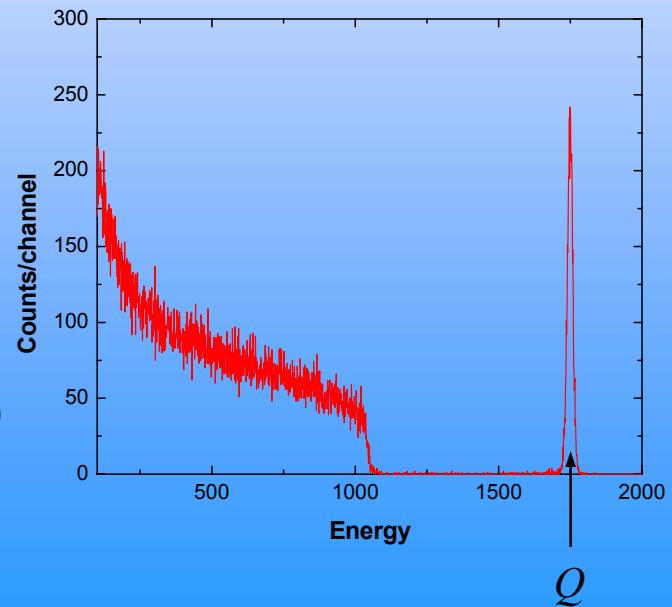
N_0 : Number of incident particles

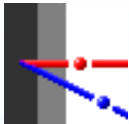
Ω : Detector solid angle

$\sigma(E)$: Differential scattering cross section (Barns/sr)

Δx : Layer thickness (Atoms/cm²)

α : Angle of incidence





RBS-Spectrum of a thin layer (2)



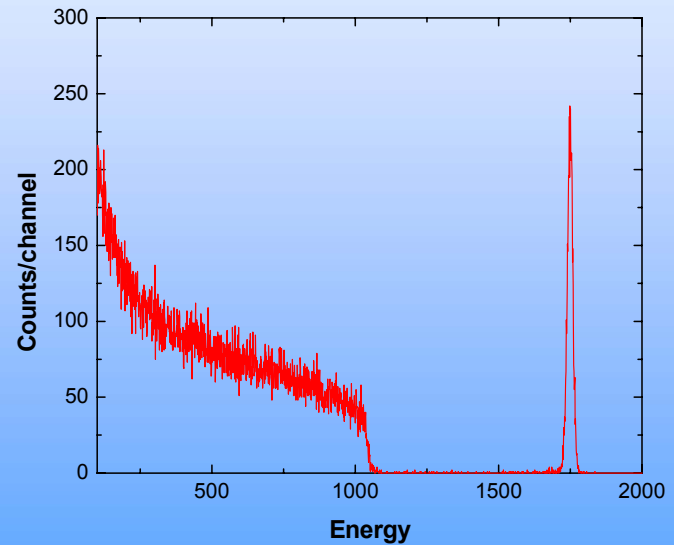
Convolution with experimental energy resolution

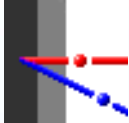
Assume Gaussian energy resolution function $f(x)$ with standard deviation w

$$f(x) = \frac{1}{\sqrt{2\pi}w} e^{-\frac{(x-x_0)^2}{2w^2}}$$

Count density function $n(E) = \frac{Q}{\sqrt{2\pi}w} e^{-\frac{(E-K E_0)^2}{2w^2}}$

Counts N_i in channel i $N_i = \int_{E_i^{Low}}^{E_i^{High}} n(E) dE$





RBS-Spectrum of a thick layer



- Target is divided into thin sublayers (“slabs”)
- Calculate backscattering from front and back side of each sublayer taking energy loss into account

Energy at front side

$$E_1 = E_0 - \Delta E_{in}$$

Starting energy from front side $E_1' = K E_1$

Energy at surface

$$E_1^{out} = E_1' - \Delta E_1^{out}$$

Energy at back side

$$E_2 = E_1 - \Delta E$$

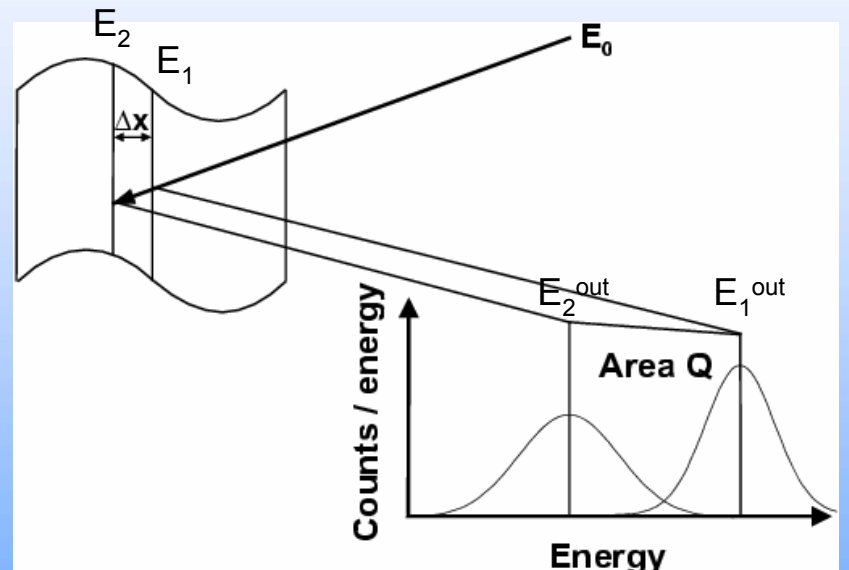
Starting energy from back side $E_2' = K E_2$

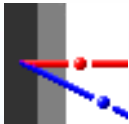
Energy at surface

$$E_2^{out} = E_2' - \Delta E_2^{out}$$

- For each isotope of each element in sublayer

⇒ “Brick”





RBS-Spectrum of a thick layer (2)



Area Q of the brick:

$$Q = N_0 \Omega \sigma(E) \frac{\Delta x}{\cos \alpha}$$

Q : Number of counts

N_0 : Number of incident particles

Ω : Detector solid angle

$\sigma(E)$: Differential scattering cross section

Δx : Thickness of sublayer (in Atoms/cm²)

α : Angle of incidence

How to determine $\sigma(E)$?

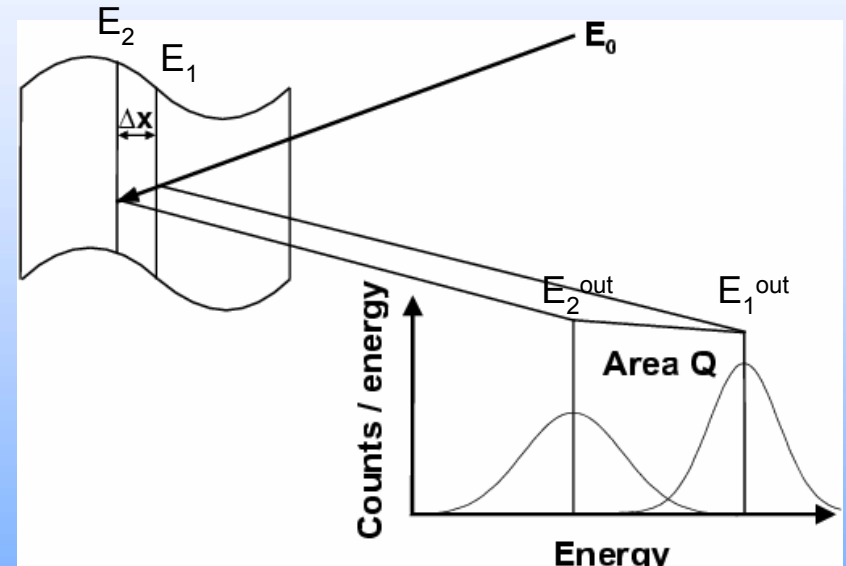
- Mean energy approximation:

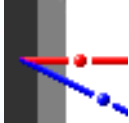
Use $\sigma(\langle E \rangle)$, with $\langle E \rangle = E_1 - \Delta E/2$

- Mean cross section $\langle \sigma \rangle$:

$$\langle \sigma \rangle = \frac{\int_{E_2}^{E_1} \sigma(E) dE}{E_1 - E_2}$$

\Rightarrow More accurate, but time consuming





RBS-Spectrum of a thick layer (3)

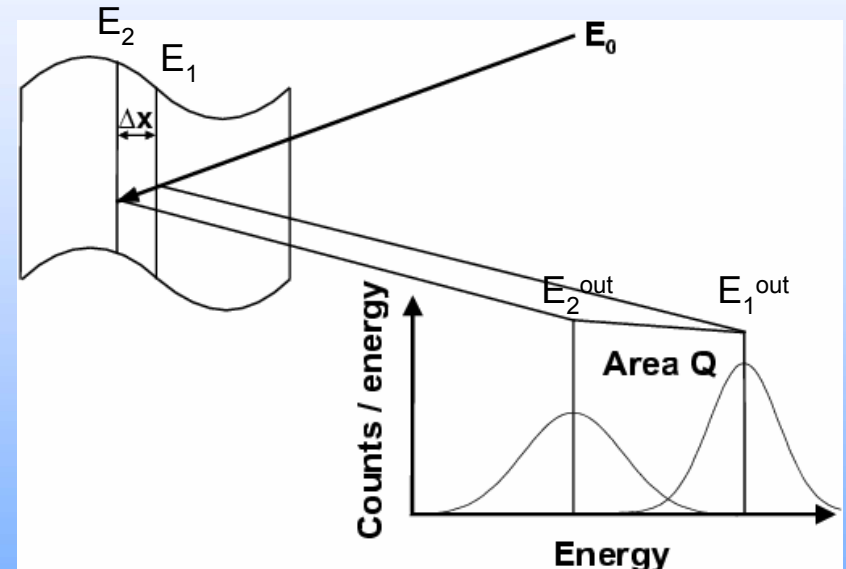


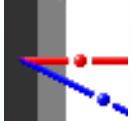
Shape of the brick:

- Height of high energy side $\propto \sigma(E_1)$
- Height of low energy side $\propto \sigma(E_2)$
- use linear interpolation

Better approximations:

- Height of high energy side $\propto \sigma(E_1)/S_{\text{eff}}(E_1)$
- Height of low energy side $\propto \sigma(E_2)/S_{\text{eff}}(E_2)$
- S_{eff} : Effective stopping power, taking stopping on incident and exit path into account
- use quadratic interpolation with additional point $\langle E \rangle$



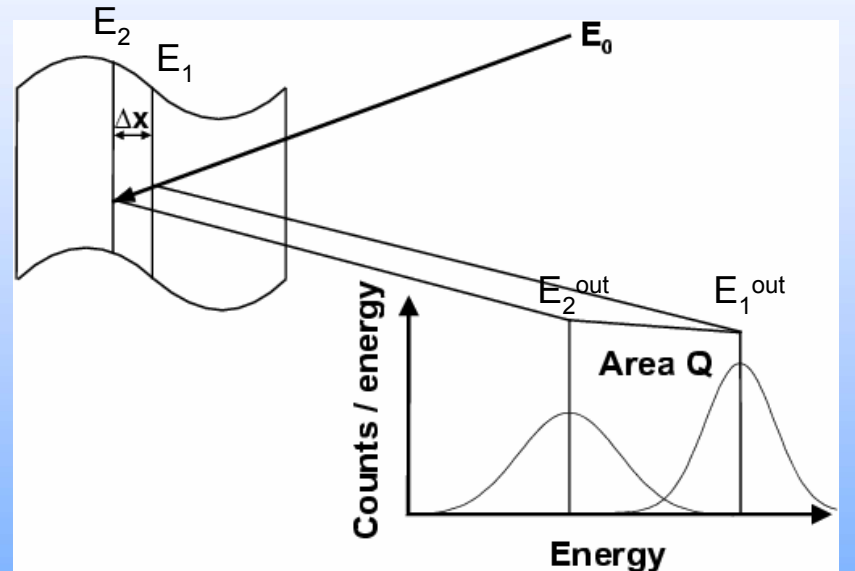
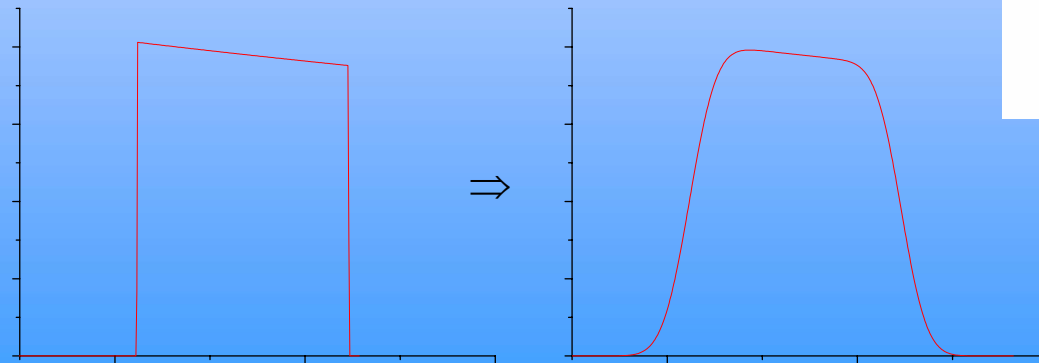


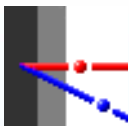
RBS-Spectrum of a thick layer (4)



Convolution of brick with energy broadening

- Detector resolution
- Energy straggling
- Depth dependent

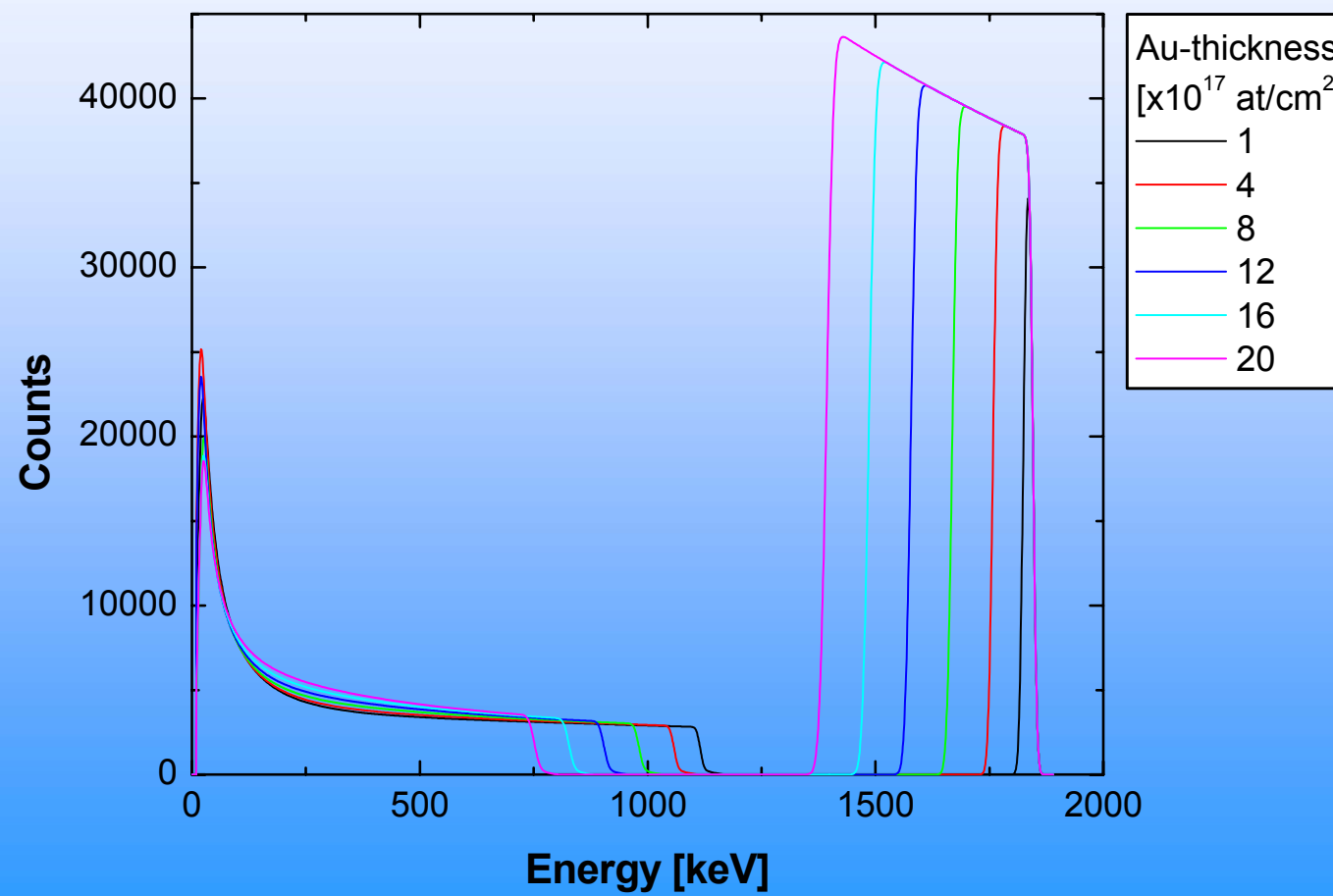


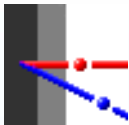


RBS-Spectrum of a thick layer: Example

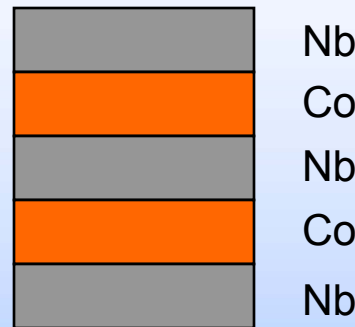
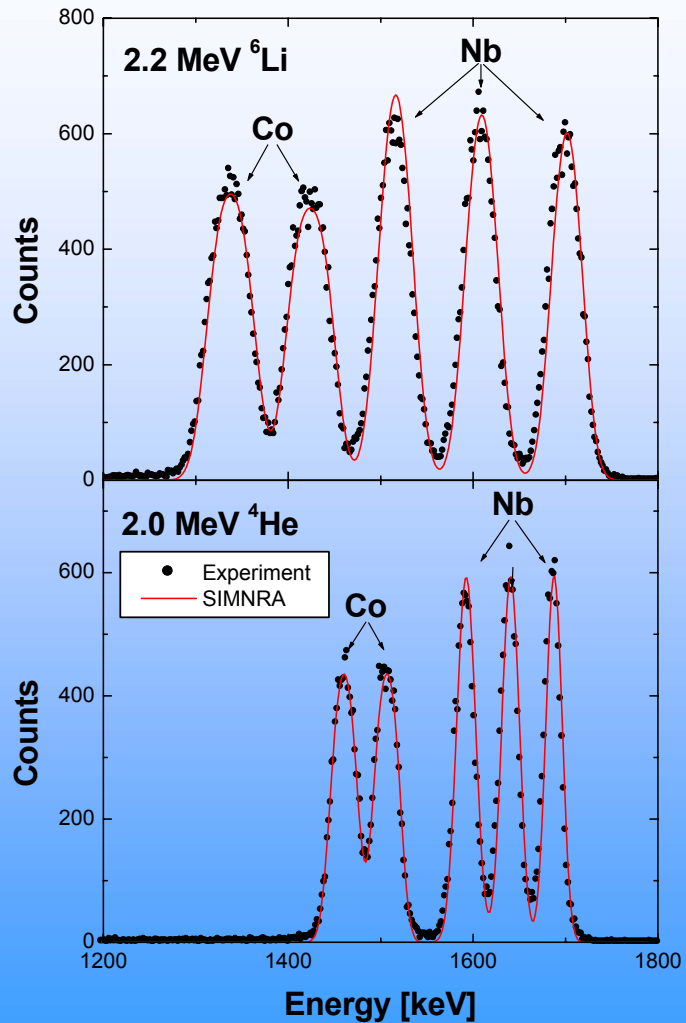
IPP

2000 keV ${}^4\text{He}$, $\theta = 165^\circ$ backscattered from Au on Si substrate



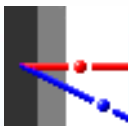


RBS-Spectra: Example (1)

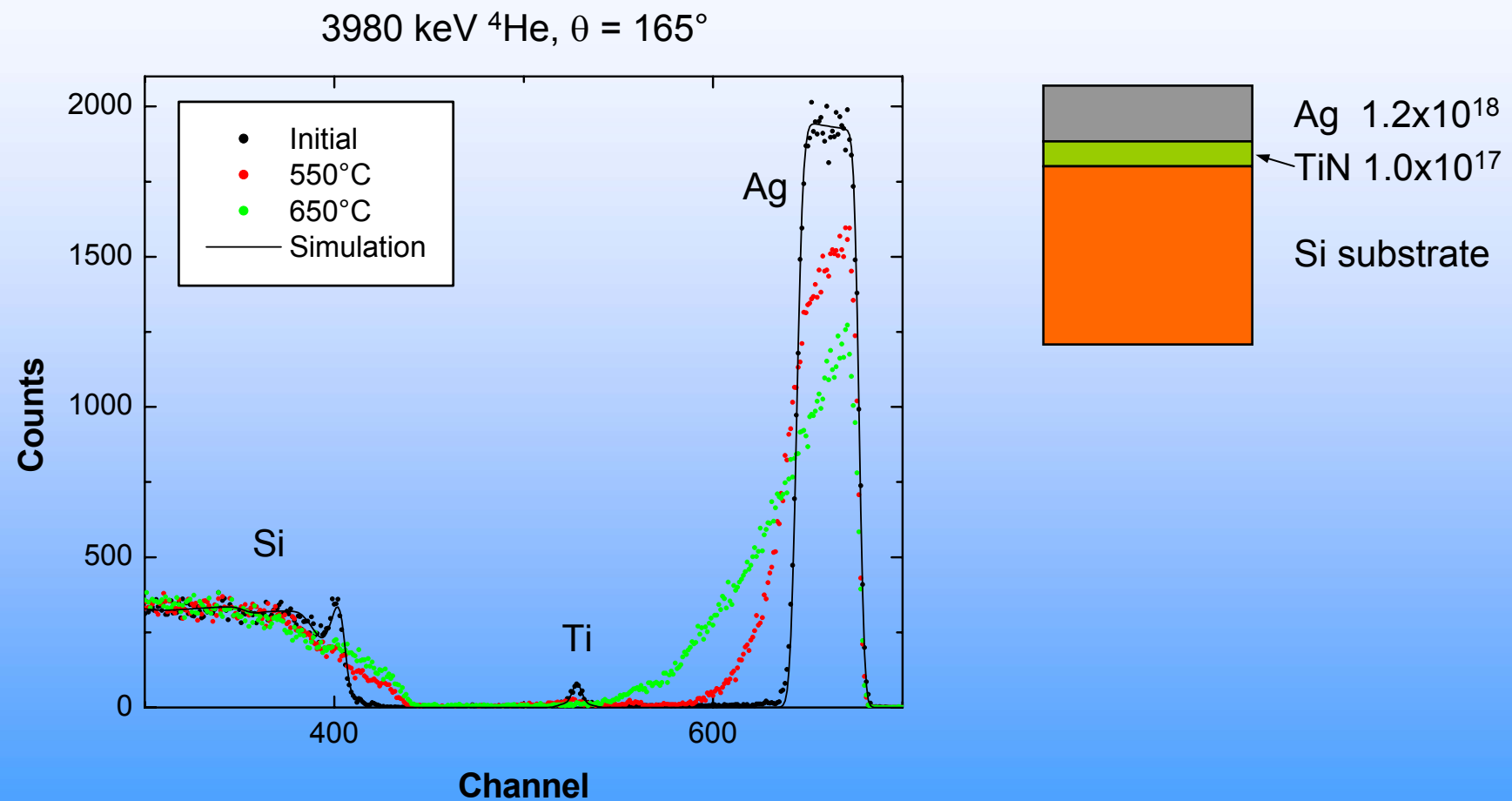


Nb: $1.0 \times 10^{17} \text{ at/cm}^2$
Co: $2.2 \times 10^{17} \text{ at/cm}^2$

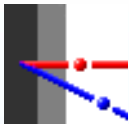
M. Mayer et al., Nucl. Instr. Meth. B190 (2002) 405



RBS-Spectra: Example (2)



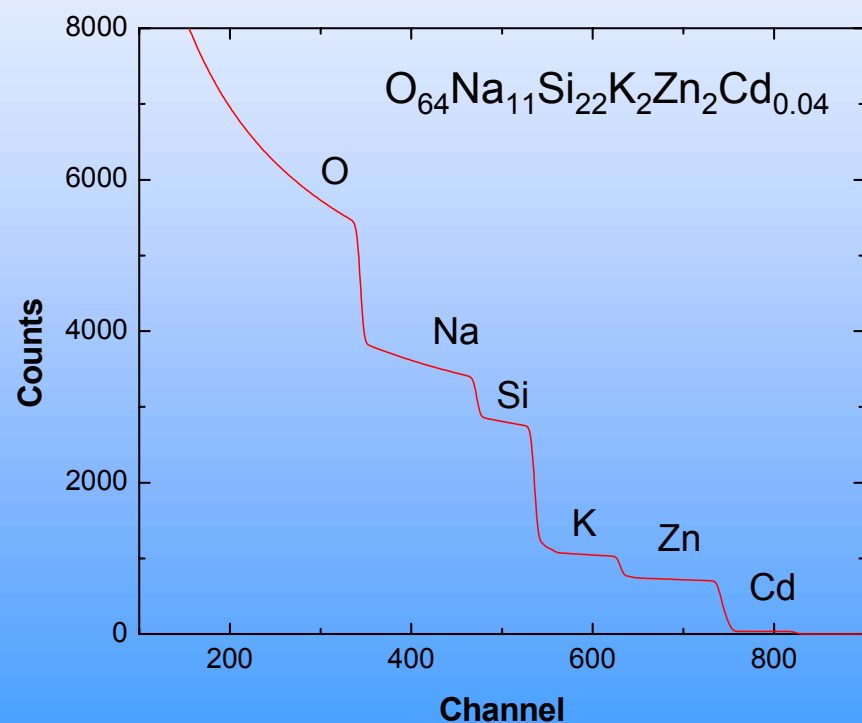
M. Balden, unpublished

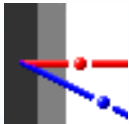


RBS-Spectra: Example (3)



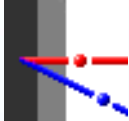
1.9 MeV ${}^4\text{He}$, 170° backscattered from ceramic glass





Index

- History
- Scattering geometry and kinematics
- Rutherford cross section and limitations
- RBS spectra from thin and thick films
- **Stopping power and energy loss**
- Detector resolution
- Energy loss straggling
- Cross sections from selected light elements
 - incident ^1H
 - incident ^4He



Stopping Power



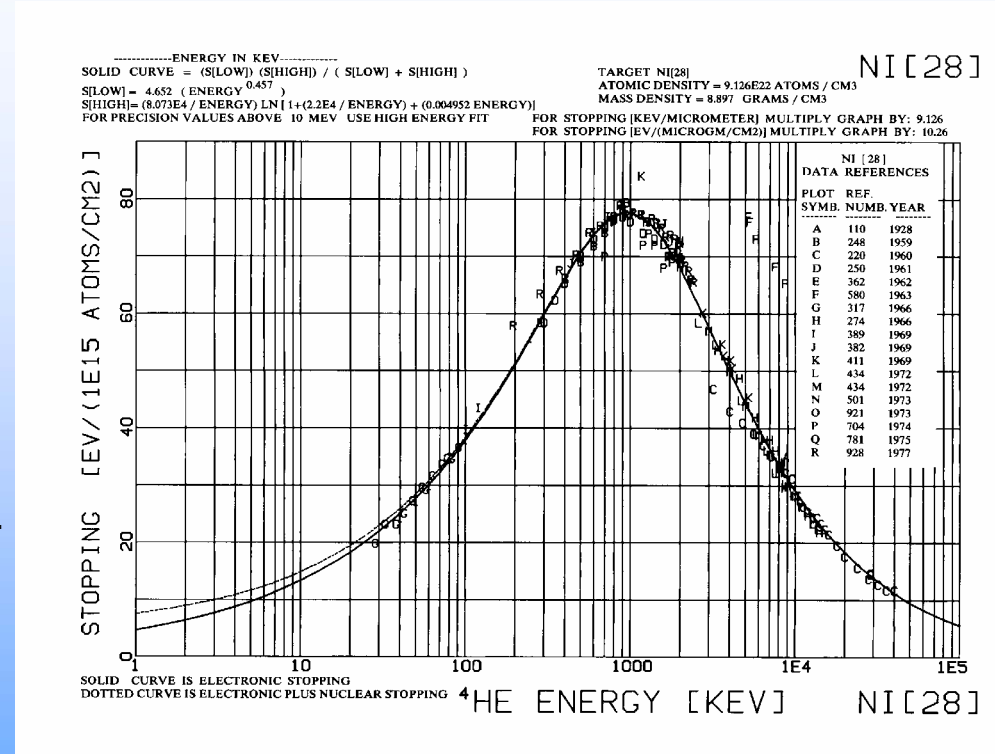
- **Electronic stopping power:**

- Andersen, Ziegler (1977):
H, He in all elements
- Ziegler, Biersack, Littmarck (1985):
All ions in all elements
- Several SRIM-versions since then
- Additional work by Kalbitzer, Paul, ...
- Accuracy: 5% for H, He
10% for heavy ions

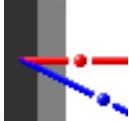
- **Nuclear stopping power:**

- Only important for heavy ions or low energies
- Ziegler, Biersack, Littmarck (1985):
All ions in all elements using ZBL potential

${}^4\text{He}$ in Ni



J.F. Ziegler, Helium - Stopping Powers and Ranges in All Elements, Vol. 4, Pergamon Press, 1977



Stopping Power (2)

Stopping in compounds:

consider compound $A_m B_n$, with $m + n = 1$

S_A is stopping power in element A

S_B is stopping power in element B

What is stopping power S_{AB} in compound?

Bragg's rule (Bragg and Kleeman, 1905):

$$S_{AB} = m S_A + n S_B$$

Bragg's rule is accurate in:

- Metal alloys

Bragg's rule is inaccurate (up to 20%) in:

- Hydrocarbons
- Oxides
- Nitrides
- ...

Other models for compounds

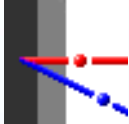
- Hydrocarbons:

Cores-and-Bonds (CAB) model

Ziegler, Manoyan (1988)

Contributions of atomic cores
and chemical bonds between atoms

- Large number of experimental data,
especially for hydrocarbons, plastics, ...



Evaluation of Energy Loss

Question: Energy $E(x)$ in depth x ?

⇒ Taylor expansion of $E(x)$ at $x = 0$:

$$E(x) = E(0) + x \frac{dE}{dx} \Big|_{x=0} + \frac{1}{2} x^2 \frac{d^2 E}{dx^2} \Big|_{x=0} + \frac{1}{6} x^3 \frac{d^3 E}{dx^3} \Big|_{x=0} + \dots$$

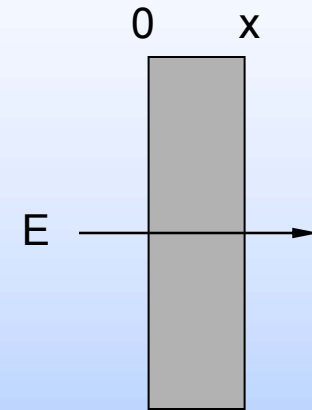
$$\frac{dE}{dx} = -S$$

S : Stopping power

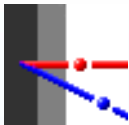
$$\frac{d^2 E}{dx^2} = \frac{d}{dx}(-S) = -\frac{dS}{dE} \frac{dE}{dx} = S'S$$

$$\frac{d^3 E}{dx^3} = \frac{d}{dx}(S'S) = \frac{dS'}{dx} S + S' \frac{dS}{dx} = -S''S^2 - S'^2 S$$

$$\Rightarrow \boxed{E(x) = E_0 - xS + \frac{1}{2} x^2 SS' - \frac{1}{6} x^3 (S''S^2 + S'^2 S) + \dots}$$



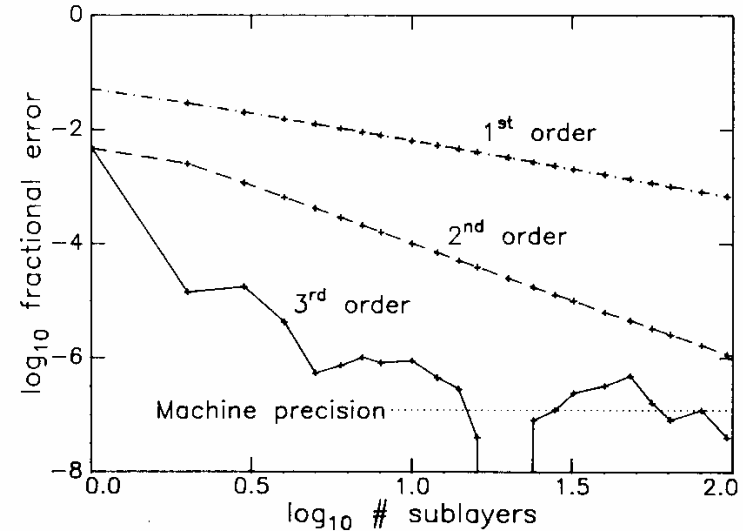
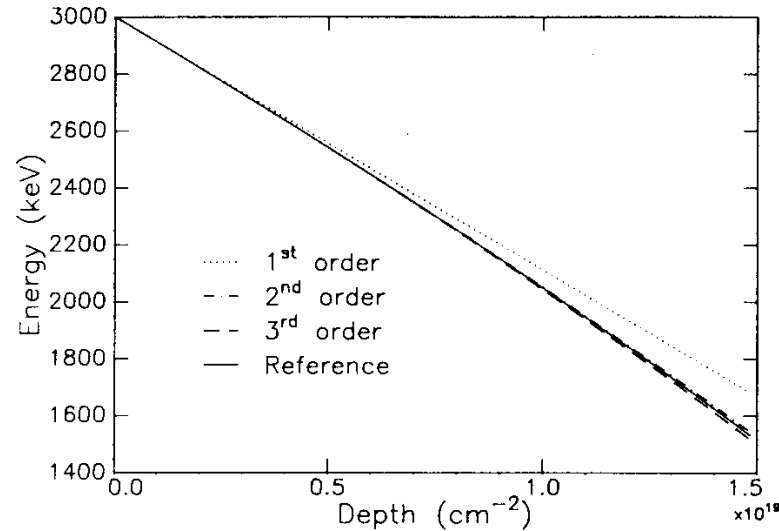
S, S', S'' evaluated at $x = 0$



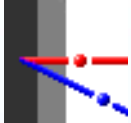
Evaluation of Energy Loss (2)

IPP

3 MeV ${}^4\text{He}$ in Pt



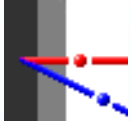
L.R. Doolittle, Nucl. Instr. Meth. B9 (1985) 344



Index

IPP

- History
- Scattering geometry and kinematics
- Rutherford cross section and limitations
- RBS spectra from thin and thick films
- Stopping power and energy loss
- **Detector resolution**
- Energy loss straggling
- Cross sections from selected light elements
 - incident ^1H
 - incident ^4He

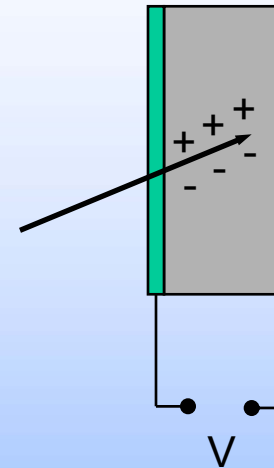


Silicon Detector Resolution

IPP

Principle of operation:

- Creation of electron-hole pairs by charged particles
- Separation of electron-hole pairs by high voltage V
 - ⇒ Number of electron-hole pairs \propto Particle energy
 - ⇒ Charge pulse \propto Particle energy

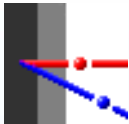


Limited energy resolution due to:

- Statistical fluctuations in energy transfer to electrons and phonons
- Statistical fluctuations in annihilation of electron-hole pairs

Additional energy broadening due to:

- Preamplifier noise
- Other electronic noise



Silicon Detector Resolution (2)

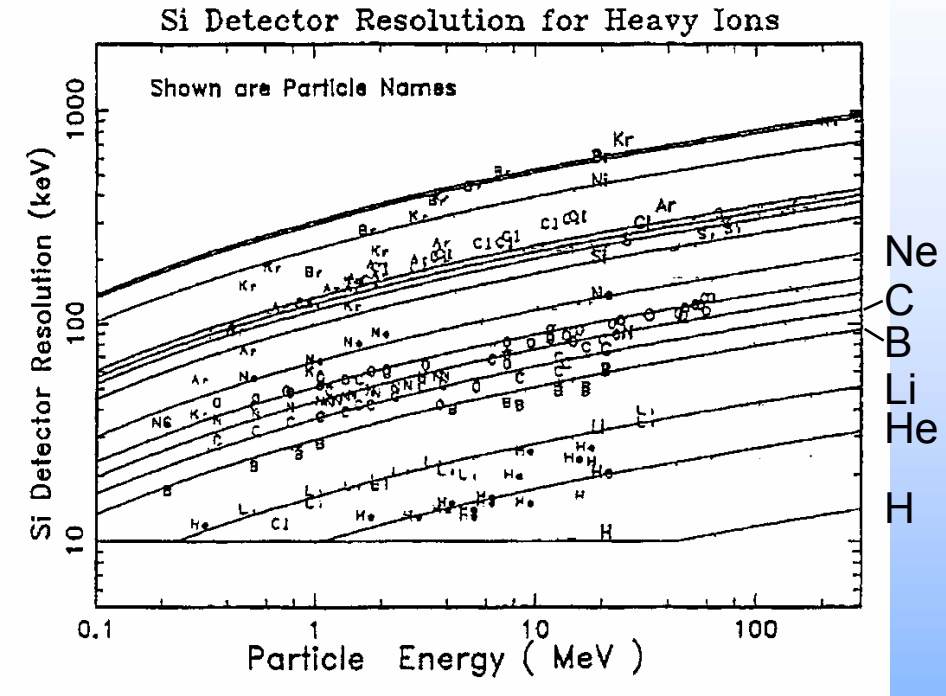
IPP

Typical values (FWHM):

- H 2 MeV: 10 keV
- He 2 MeV: 12 keV
- Li 5 MeV: 20 keV

Ad-hoc fit to experimental data:

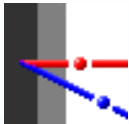
$$\text{FWHM resolution (keV)} = C_1(Z_1)^{C_2} (\ln E_{\text{keV}})^{C_3} - C_4(Z_1)^{C_5} / (\ln E_{\text{keV}})^{C_6}$$
$$C_n = 0.0999288, 1.1871, 1.94699, 0.18, 2.70004, 9.29965$$



J.F. Ziegler, Nucl. Instr. Meth. B136-138 (1998) 141

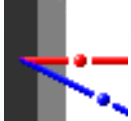
Better energy resolution for heavy ions can be obtained by:

- Electrostatic analyser (Disadvantage: large)
- Magnetic analyser (Disadvantage: large)
- Time-of-flight (Disadvantage: length, small solid angle)



Index

- History
- Scattering geometry and kinematics
- Rutherford cross section and limitations
- RBS spectra from thin and thick films
- Stopping power and energy loss
- Detector resolution
- **Energy loss straggling**
- Cross sections from selected light elements
 - incident ^1H
 - incident ^4He

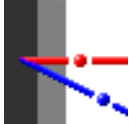


Energy Straggling

IPP

Slowing down of ions in matter is accompanied by a spread of beam energy
⇒ **energy straggling**

- **Electronic energy loss straggling** due to statistical fluctuations in the transfer of energy to electrons
- **Nuclear energy loss straggling** due to statistical fluctuations in the nuclear energy loss
- **Geometrical straggling** due to finite detector solid angle and finite beam spot size
- **Multiple small angle scattering**
- **Surface and interlayer roughness**



Electronic Energy Loss Straggling

Due to **statistical fluctuations** in the transfer of energy to electrons

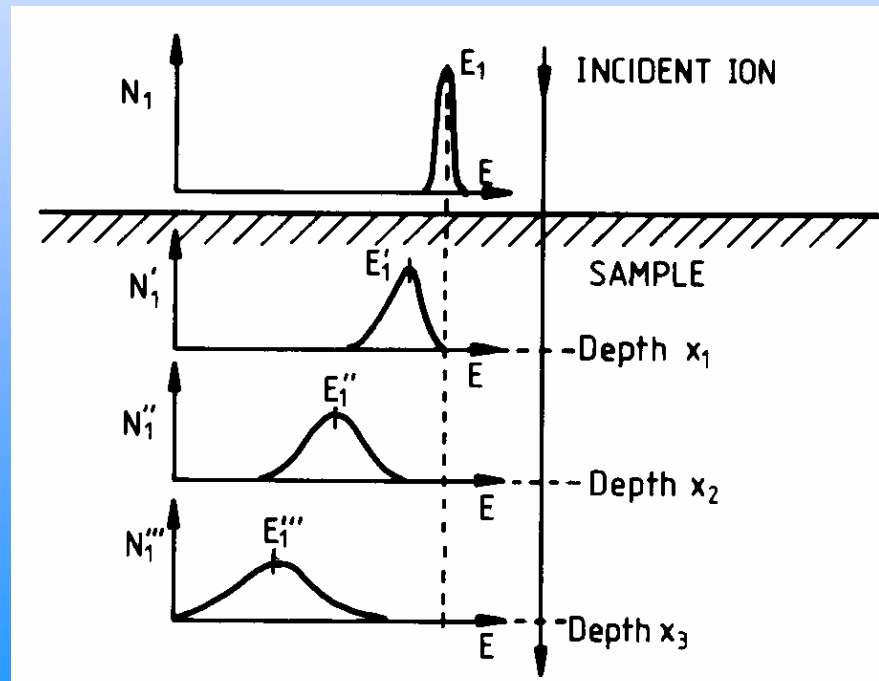
⇒ statistical fluctuations in energy loss

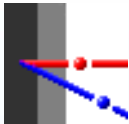
Energy after penetrating a layer Δx : $\langle E \rangle = E_0 - S \Delta x$

$\langle E \rangle$ mean energy

S stopping power

⇒ **only applicable for mean energy of many particles**



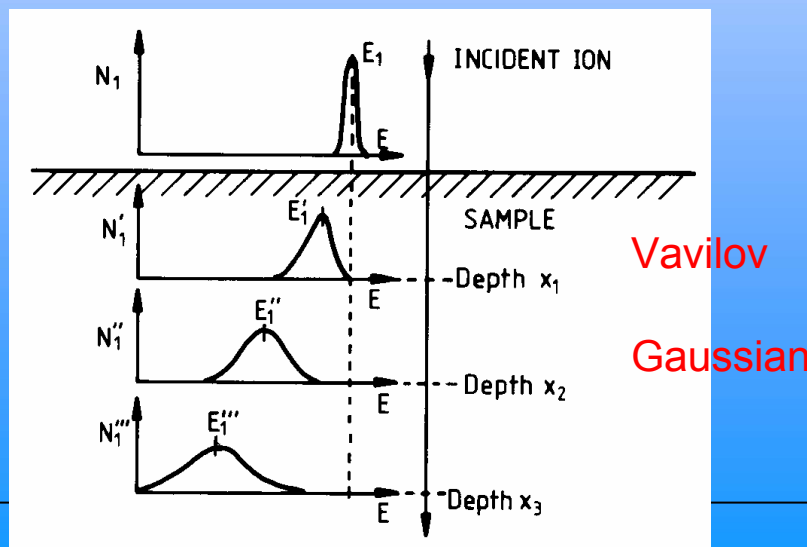


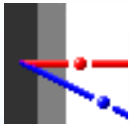
Electronic Energy Loss Straggling (2)

IPP

Shape of the energy distribution?

$\Delta E/E_0$		
< 10%	Vavilov theory	Low number of ion-electron collisions Non-Gaussian
10% – 20%	Bohr theory	Large number of ion-electron collisions Gaussian
20% – 50%	Symon theory	Non-stochastic broadening due to stopping Almost Gaussian
50% – 90%	Payne, Tschalär theory	Energy below stopping power maximum Non stochastic squeezing due to stopping Non-Gaussian





Vavilov Theory

IPP

Vavilov 1957

P.V. Vavilov, Soviet Physics J.E.T.P. **5** (1957) 749

Valid for small energy losses

⇒ Low number of ion-electron collisions

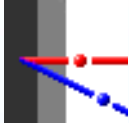
⇒ Non-Gaussian energy distribution with tail towards low energies



Mostly replaced by Bohr's theory and approximated by Gaussian distribution

⇒ Total energy resolution near the surface usually dominated by detector resolution
due to small energy loss straggling

⇒ Only necessary in high resolution experiments



Bohr Theory

Bohr 1948

N. Bohr, Mat. Fys. Medd. Dan. Vid. Selsk. **18** (1948)

Valid for intermediate energy losses

- ⇒ Large number of ion-electron collisions
- ⇒ Gaussian energy distribution

Approximations in Bohr's theory:

- Ions penetrating a gas of free electrons
- Ions are fully ionised
- Ion velocity \gg electron velocity ⇒ stationary electrons
- Stopping power effects are neglected

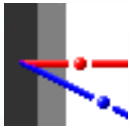
$$\sigma_{Bohr}^2 = 0.26 Z_1^2 Z_2 \Delta x$$

σ_{Bohr}^2 variance of the Gaussian distribution [keV²]

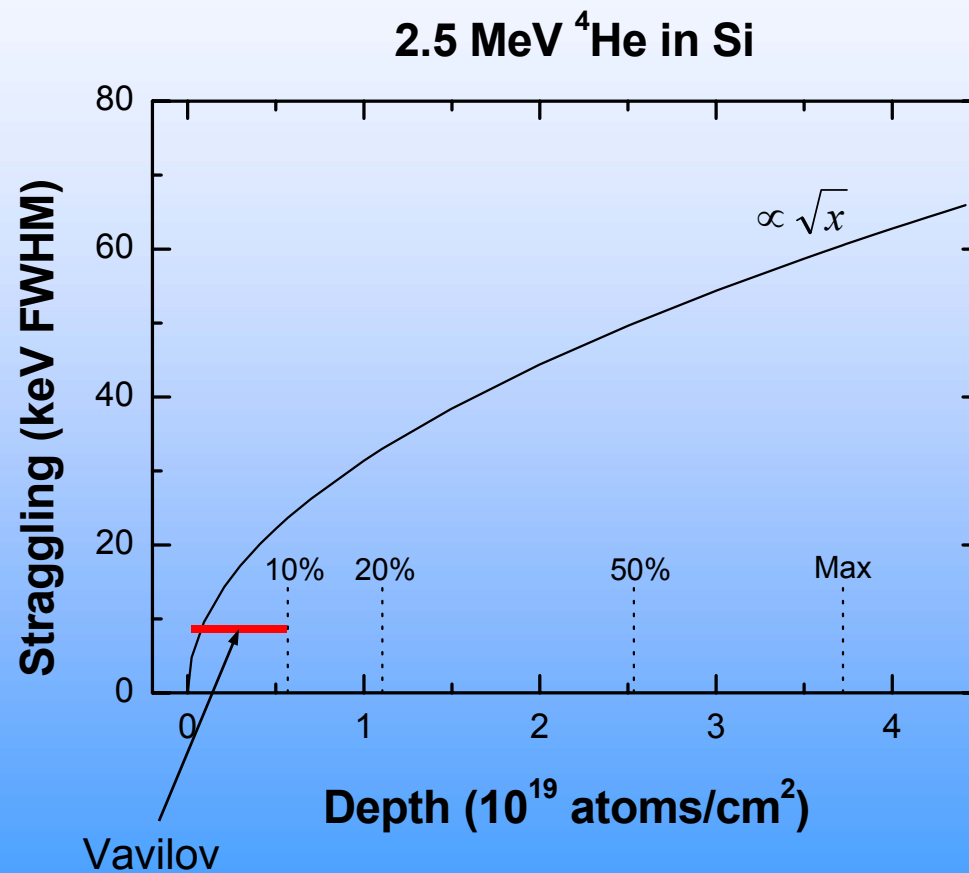
Δx depth [10^{18} atoms/cm²]

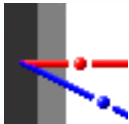
Z_1 atomic number of incident ions

Z_2 atomic number of target atoms



Bohr Theory: Example





Improvements to Bohr Theory



Chu 1977

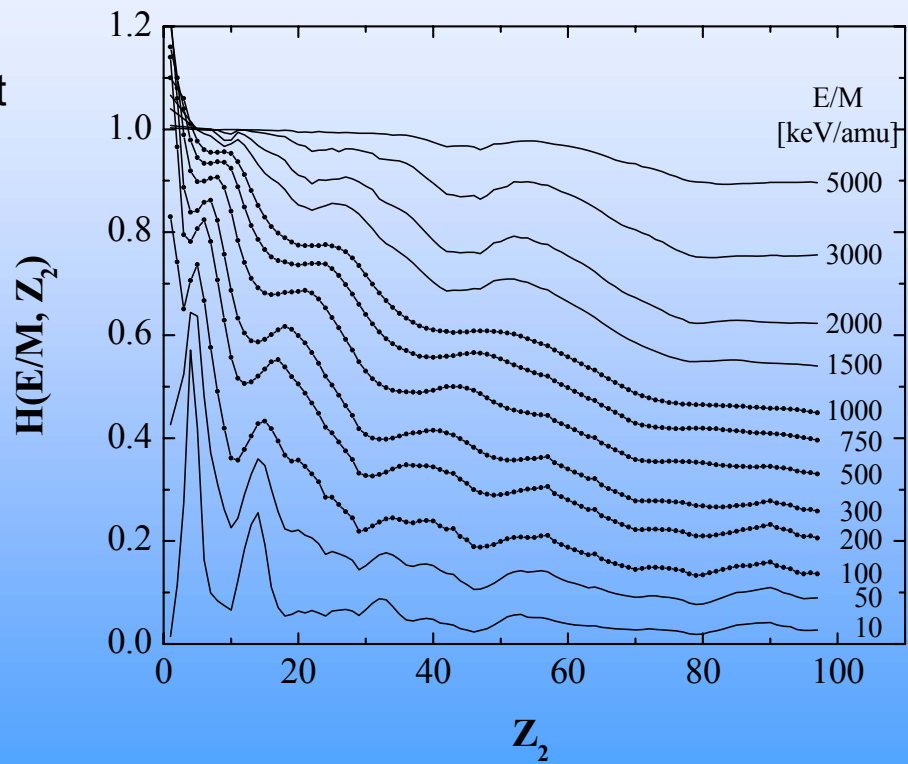
J.W. Mayer, E. Rimini, Ion Beam Handbook for Material Analysis, 1977

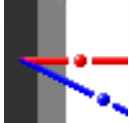
Approximations in Chu's theory:

- Binding of electrons is taken into account
- Hartree-Fock electron distribution
- Stopping power effects are neglected

$$\sigma_{Chu}^2 = H\left(\frac{E}{M_1}, Z_2\right) \sigma_{Bohr}^2$$

⇒ Smaller straggling than Bohr





Straggling in Compounds

Additive rule proposed by Chu 1977

J.W. Mayer, E. Rimini, Ion Beam Handbook for Material Analysis, 1977

consider compound $A_m B_n$, with $m + n = 1$

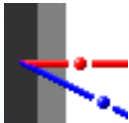
σ_A^2 is variance of straggling in element A

σ_B^2 is variance of straggling in element B

$$\sigma_{AB}^2 = \sigma_A^2 + \sigma_B^2$$

σ_A^2 Straggling in element A in a layer $m \Delta x$

σ_B^2 Straggling in element B in a layer $n \Delta x$



Propagation of Straggling in Thick Layers

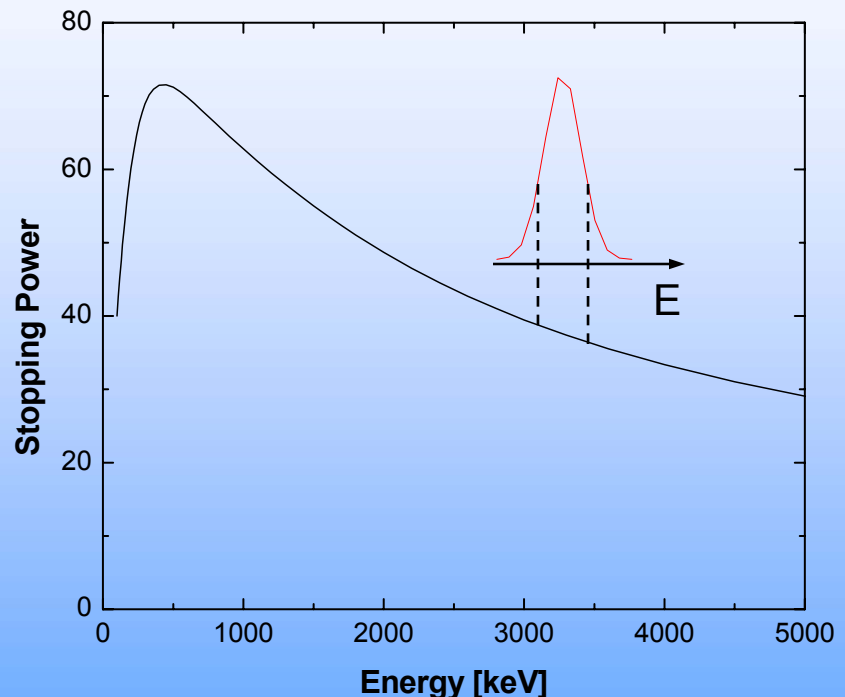
IPP

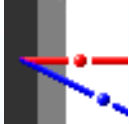
Consider particles with energy distribution

- **Energy above stopping power maximum**
higher energetic particles \Rightarrow smaller stopping
 \Rightarrow non-stochastic broadening
- **Energy below stopping power maximum**
higher energetic particles \Rightarrow larger stopping
 \Rightarrow non-stochastic squeezing

C. Tschalär, Nucl. Instr. Meth. **61** (1968) 141

M.G. Payne, Phys. Rev. **185** (1969) 611





Propagation of Straggling in Thick Layers (2)



$$E_2 = E_1 + \delta E$$

$$E_2^* = E_2 - \int_0^{\delta x} S(E(y))dy - \int_{\delta x}^x S(E(y))dy$$

$$= E_1 - \int_{\delta x}^x S(E(y))dy$$

$$\delta x \approx \frac{\delta E}{S_i}$$

Select δx so, that
 E_2 decreases to E_1

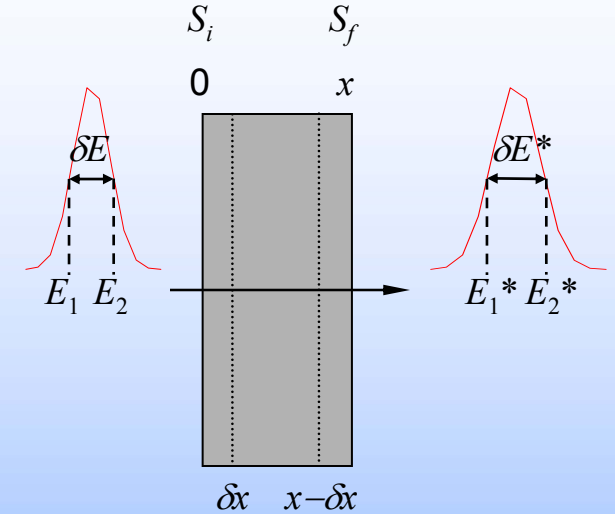
$$E_1^* = E_1 - \int_0^{x-\delta x} S(E(y))dy - \int_{x-\delta x}^x S(E(y))dy$$

$$\delta E^* = E_2^* - E_1^*$$

$$= \int_{x-\delta x}^x S(E(y))dy \\ \approx S_f \delta x$$

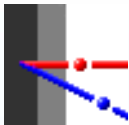
\Rightarrow

$$\delta E^* = \frac{S_f}{S_i} \delta E$$

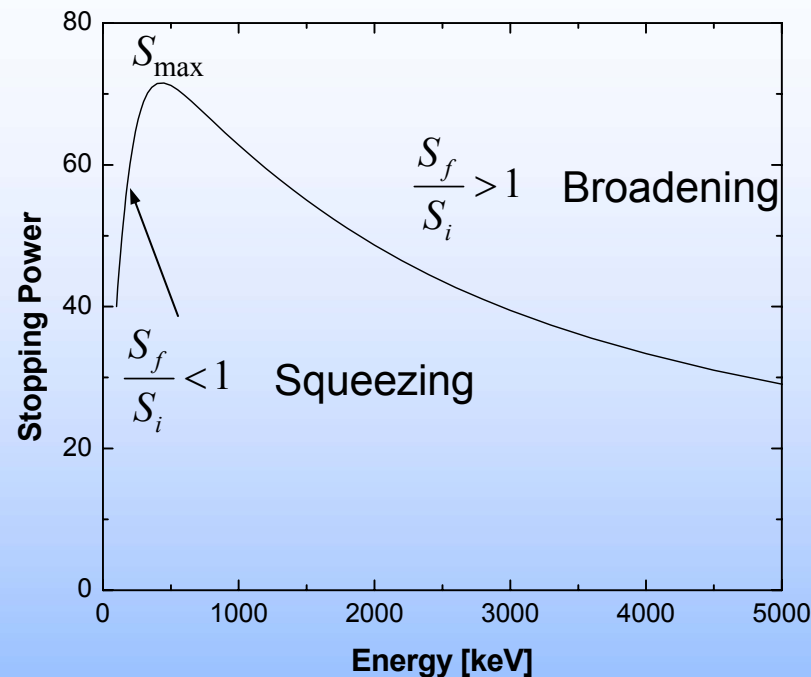


S_f Final stopping power

S_i Initial stopping power



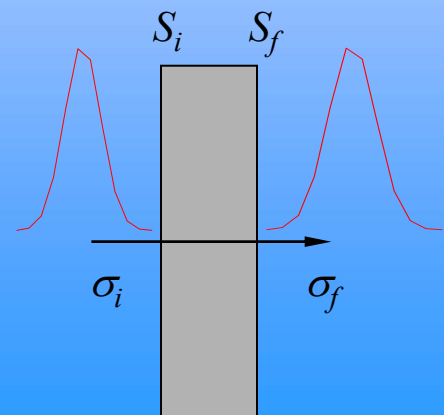
Propagation of Straggling in Thick Layers (3)

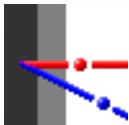


Adding stochastic and non-stochastic effects:

- Statistically independent

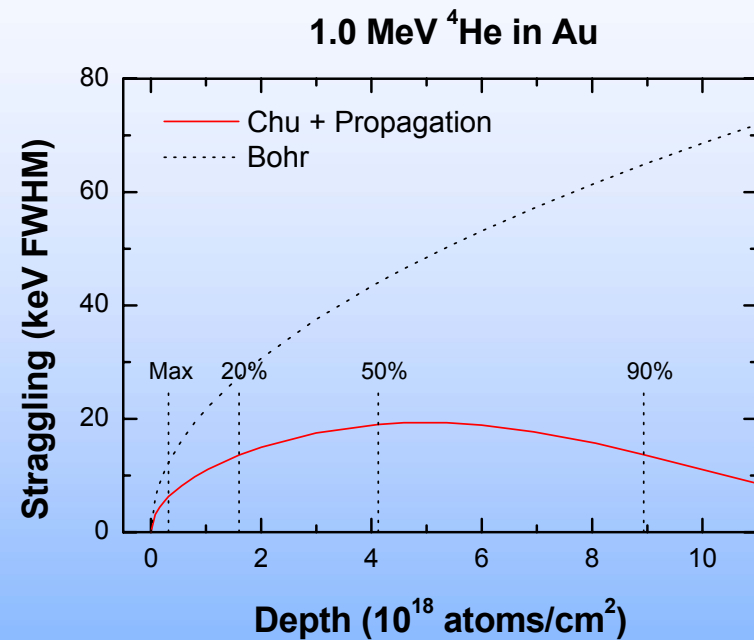
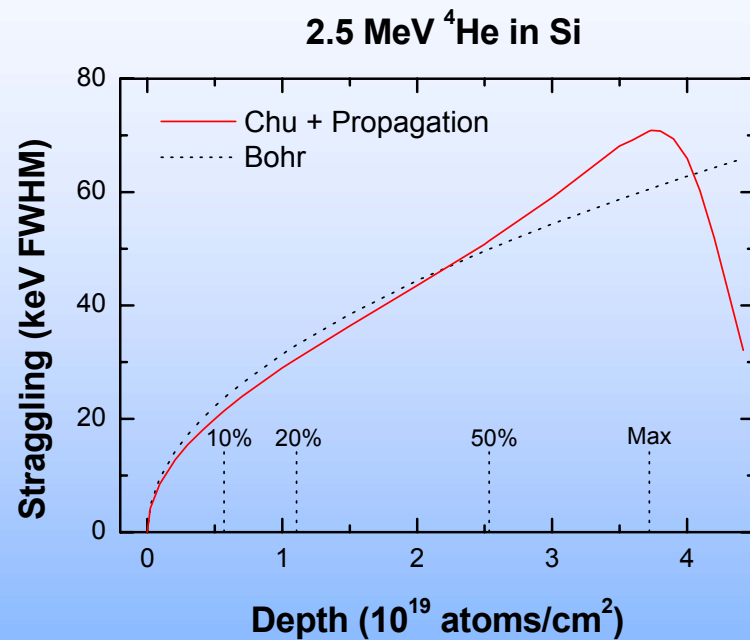
$$\sigma_f^2 = \left(\frac{S_f}{S_i} \right)^2 \sigma_i^2 + \sigma_{Chu}^2$$



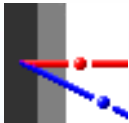


Propagation of Straggling: Examples

IPP



$$\sigma_f^2 = \left(\frac{S_f}{S_i} \right)^2 \sigma_i^2 + \sigma_{Chu}^2$$

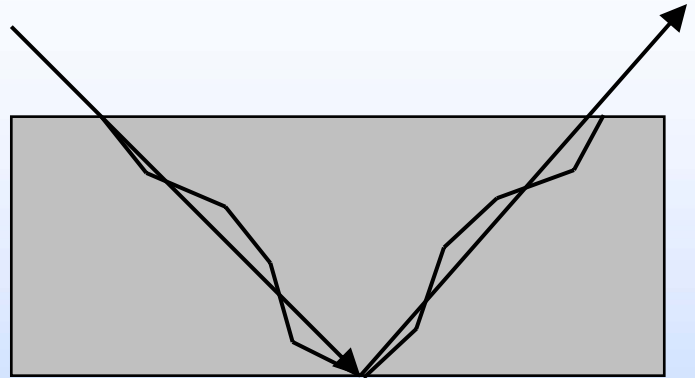


Multiple and Plural Scattering

IPP

Multiple small angle deflections

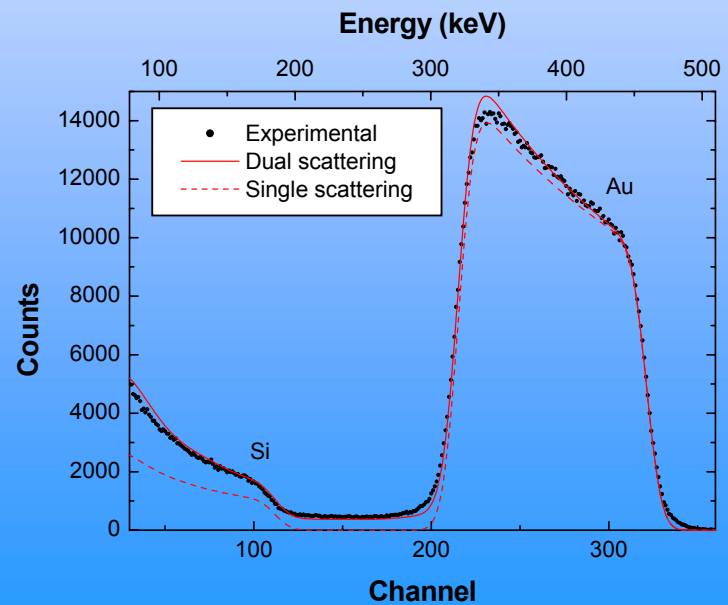
- Path length differences on ingoing and outgoing paths
⇒ energy spread
- Spread in scattering angle
⇒ energy spread of starting particles



P. Sigmund and K. Winterbon, Nucl. Instr. Meth. **119** (1974) 541

E. Szilagy et al., Nucl. Instr. Meth. **B100** (1995) 103

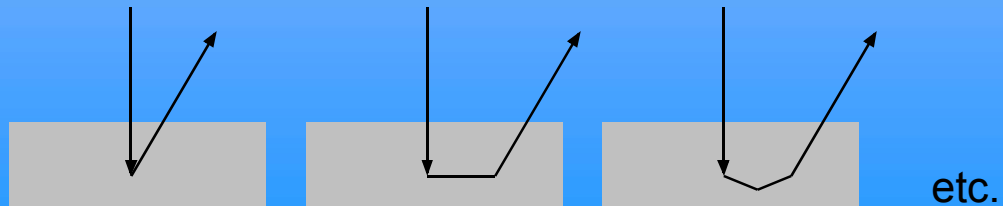
500 keV ${}^4\text{He}$, 100 nm Au on Si, $\theta = 165^\circ$

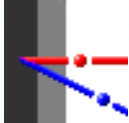


Large angle deflections (Plural scattering)

- For example: Background below high-Z layers

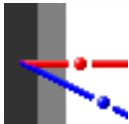
W. Eckstein and M. Mayer, Nucl. Instr. Meth. **B153** (1999) 337





Index

- History
- Scattering geometry and kinematics
- Rutherford cross section and limitations
- RBS spectra from thin and thick films
- Stopping power and energy loss
- Detector resolution
- Energy loss straggling
- **Cross sections from selected light elements**
 - incident ^1H
 - incident ^4He



Threshold for Non-Rutherford Scattering

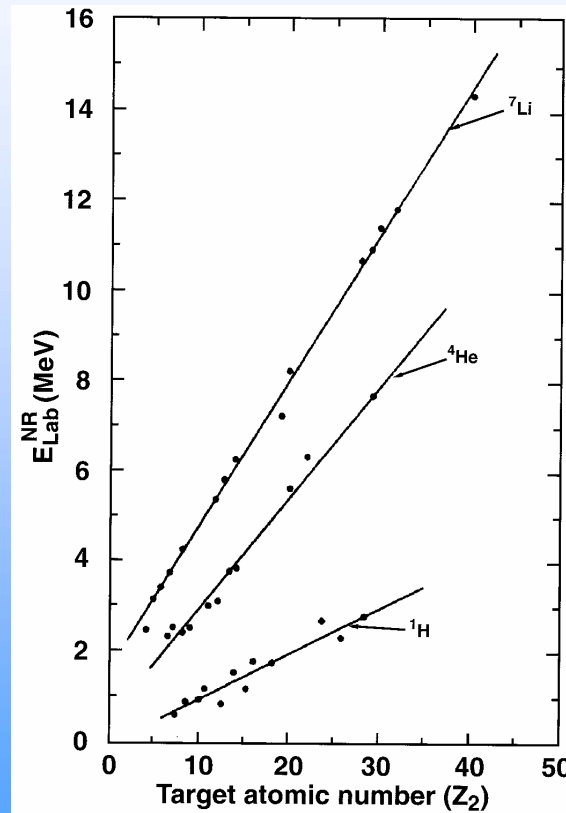
IPP

Thresholds for non-Rutherford scattering [MeV]

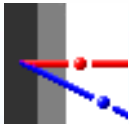
- For ^1H : $E \approx 0.12 Z_2 - 0.5$
- For ^4He : $E \approx 0.25 Z_2 + 0.4$

Z_2 for Non-Rutherford scattering

	^1H	^4He
1 MeV	12	3
2 MeV	21	6



J.R. Tesmer and M. Nastasi,
Handbook of Modern Ion Beam Materials Analysis,
MRS, 1995



Non-Rutherford Scattering: Example

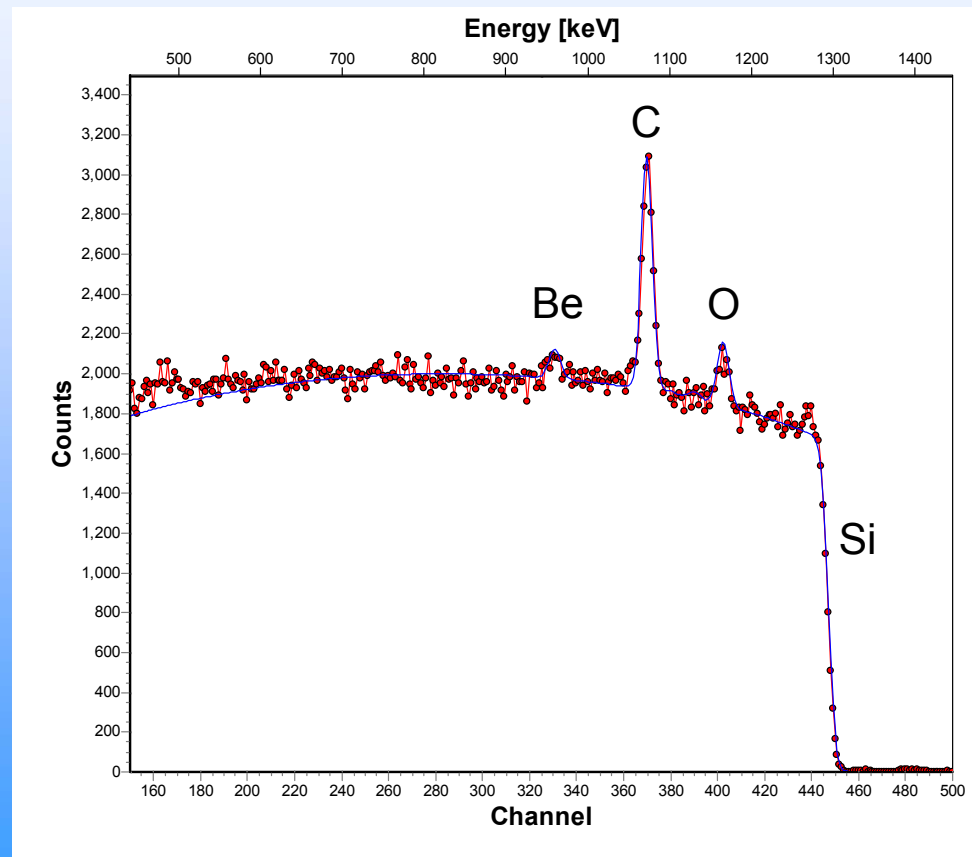
IPP

1.5 MeV H, $\theta = 165^\circ$
 6×10^{17} at/cm² Be, C, O on Si

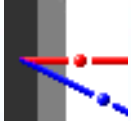
Typical problem for light elements:

Overlap with thick layers of heavier elements

⇒ **High cross sections wishful**

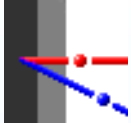


M. Mayer, unpublished



Cross Section Data Sources

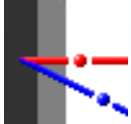
- Many non-Rutherford scattering cross sections were **measured in the years 1950 - 1970** for nuclear physics research
 - ⇒ goal was nuclear physics, not materials analysis
 - ⇒ most data published only in graphical form
- Since **1980 - to now** non-Rutherford scattering cross sections are measured for RBS analysis
 - ⇒ some data published in graphical form and tabular form
 - ⇒ for typical angles of RBS
- **Data compilation by R.A. Jarjis, Nuclear Cross Section Data for Surface Analysis**, University of Manchester, UK 1979
 - 2 volumes, 600 pages → unpublished
 - still the most comprehensive compilation of cross section data (RBS + NRA)



Cross Section Data Sources (2)

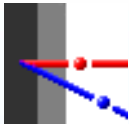


- **Data compilation by R.P. Cox et al.** for J.R. Tesmer and M. Nastasi,
Handbook of Modern Ion Beam Analysis, MRS 1995
Digitised (or tabulated) data from original publications in RTR file format
- These data are **available at SigmaBase**:
ibaserver.physics.iwu.edu/sigmabase/ or www.mfa.kfki.hu/sigmabase/
Also included in the computer code **SIMNRA**
- **Data compilation by M. Mayer** since 1996
Digitised (or tabulated) data from original publications (or authors)
in R33 file format
Most of these data are available at SigmaBase
Included in the computer code **SIMNRA**



Index

- History
- Scattering geometry and kinematics
- Rutherford cross section and limitations
- RBS spectra from thin and thick films
- Stopping power and energy loss
- Detector resolution
- Energy loss straggling
- Cross sections from selected light elements
 - incident ^1H
 - incident ^4He



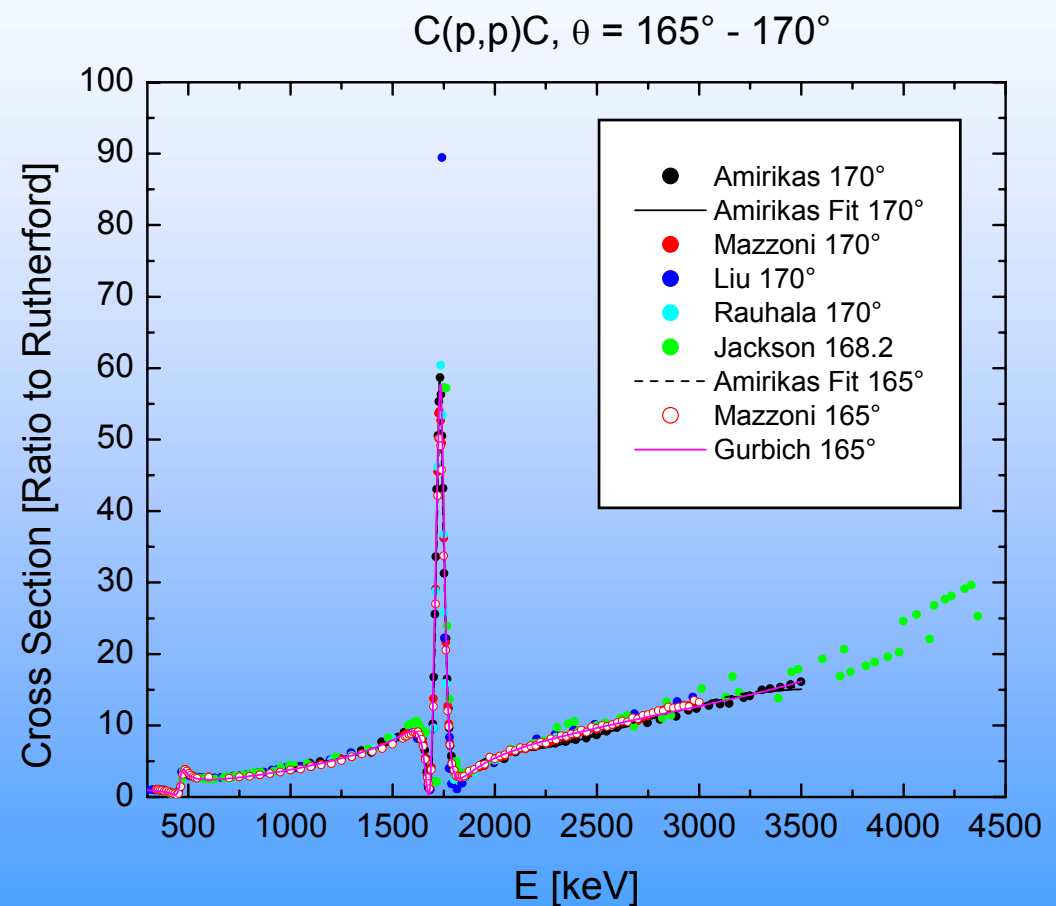
$^{12}\text{C}(\text{p},\text{p})^{12}\text{C}$

IPP

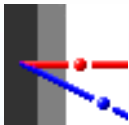
High to very high cross section
above 500 keV

Typical energies for RBS:

- 1500 or 2500 keV
 - ⇒ smooth cross section
 - ⇒ easy data evaluation, thick layers
- ≈ 1740 keV
 - ⇒ maximum sensitivity



SIMNRA Home Page <http://www.rzg.mpg.de/~mam>

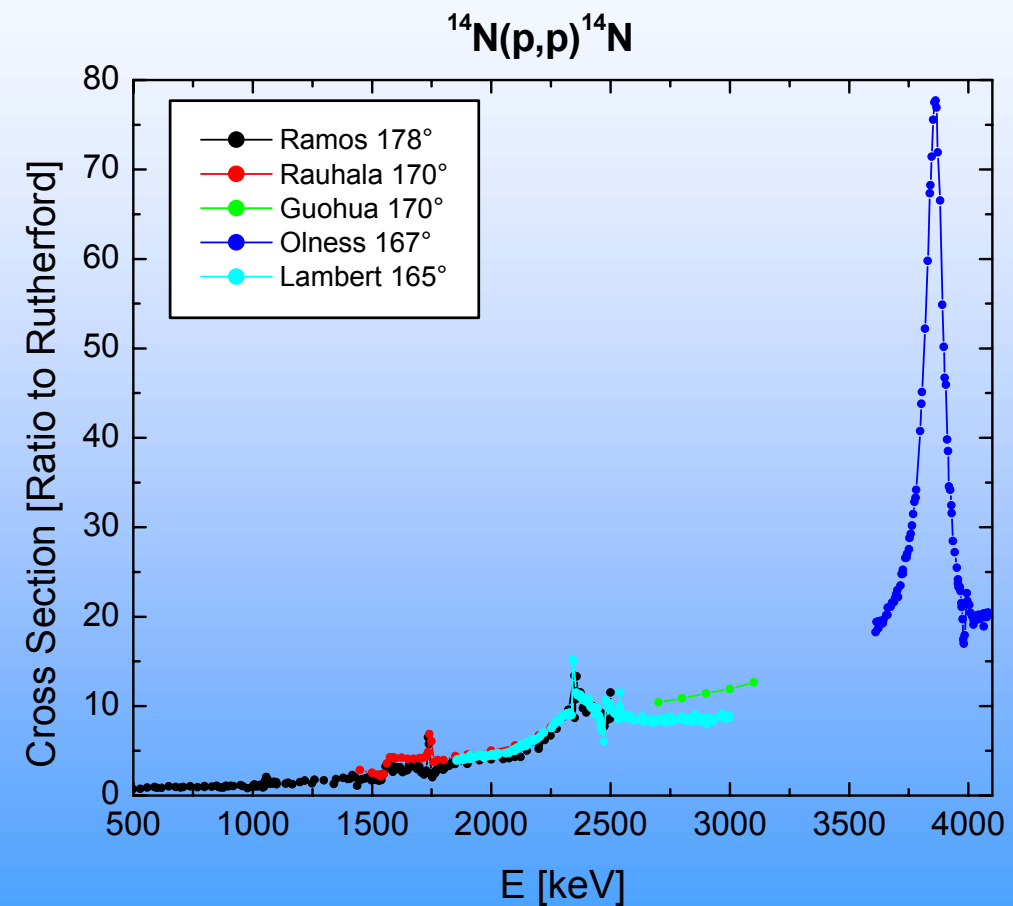


$^{14}\text{N}(\text{p},\text{p})^{14}\text{N}$

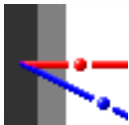
IPP

High to very high cross section

but: large scatter of data



SIMNRA Home Page <http://www.rzg.mpg.de/~mam>



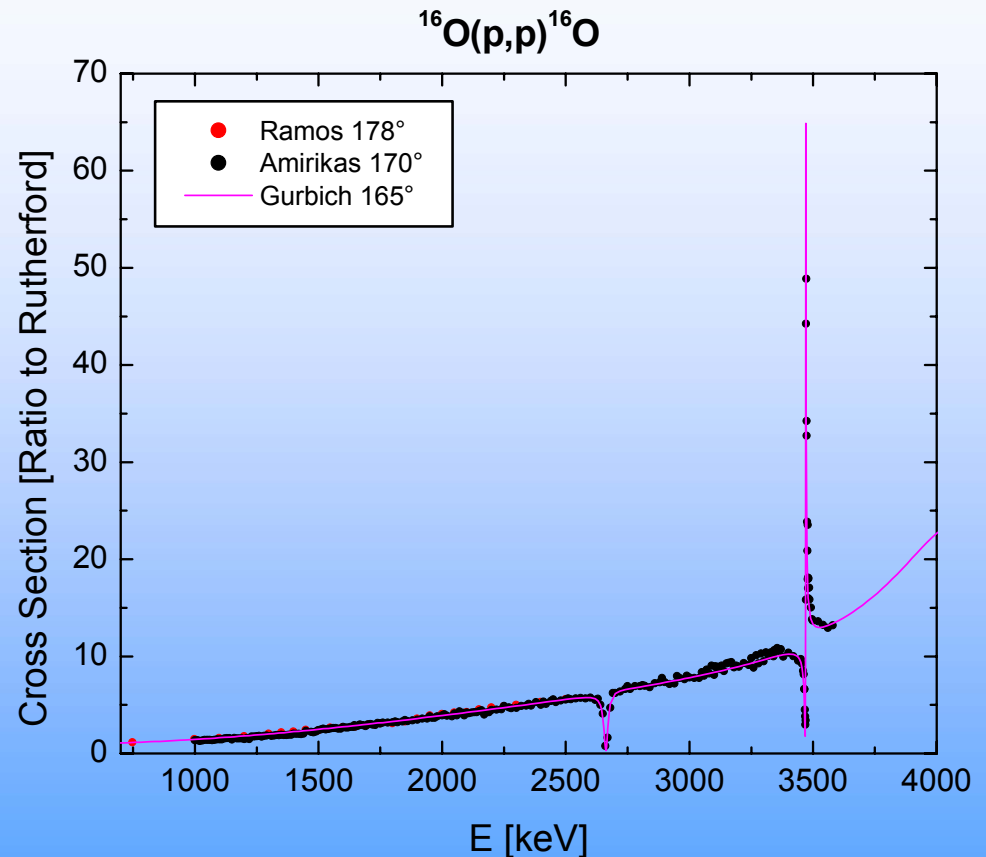
$^{16}\text{O}(\text{p},\text{p})^{16}\text{O}$

IPP

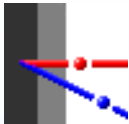
High to very high cross section

Typical energies for RBS:

- 1500 or 2500 keV
 - ⇒ smooth cross section
 - ⇒ together with C
- ≈ 3470 keV
 - ⇒ maximum sensitivity



SIMNRA Home Page <http://www.rzg.mpg.de/~mam>



$^{27}\text{Al}(\text{p},\text{p})^{27}\text{Al}$

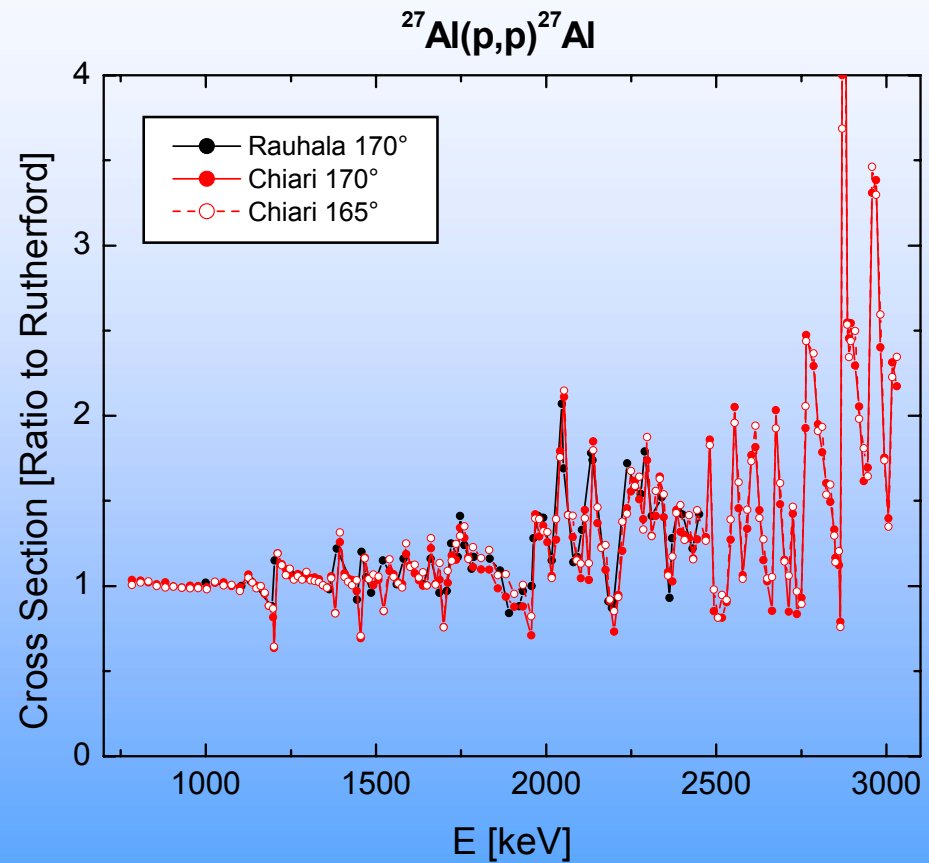
IPP

Small cross section

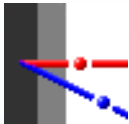
Many resonances

⇒ complicated spectrum

Not useful for RBS with protons



SIMNRA Home Page <http://www.rzg.mpg.de/~mam>



Si(p,p)Si



Small cross section

⇒ advantageous if used as substrate

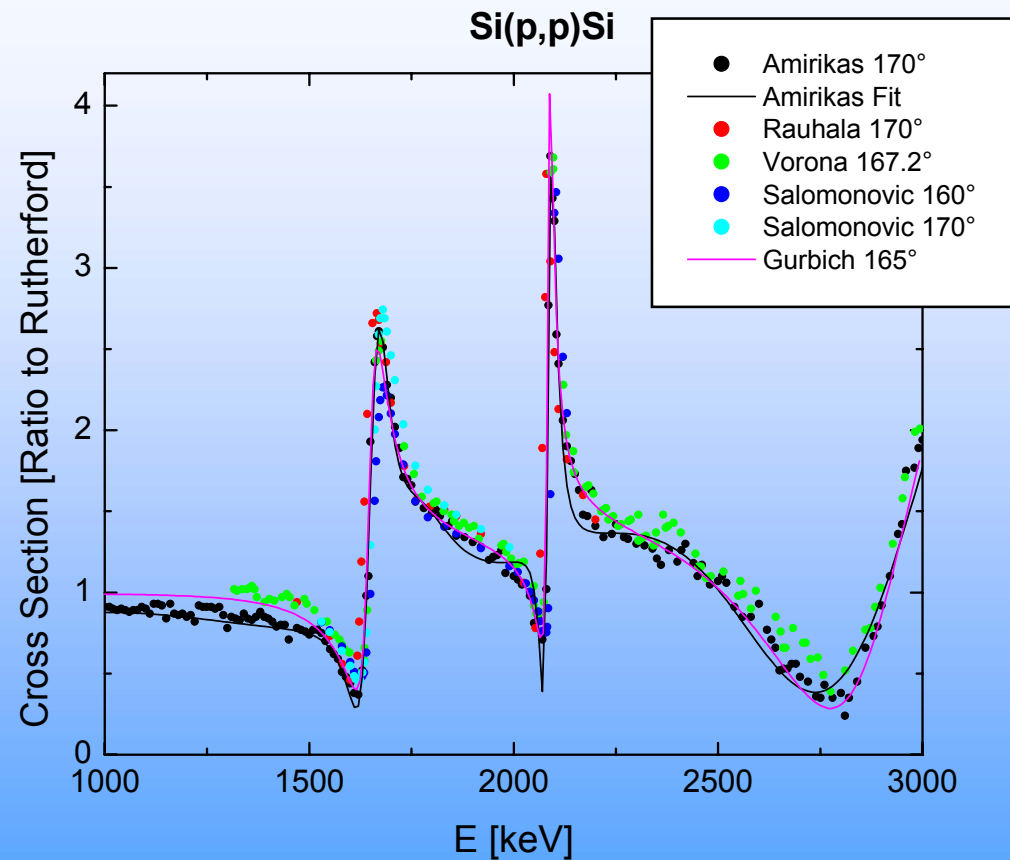
Typical energies for RBS:

- 1500 - 1600 keV

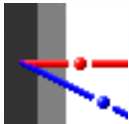
⇒ small background from substrate

- 1670 or 2090 keV

⇒ maximum sensitivity

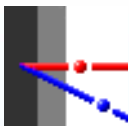


SIMNRA Home Page <http://www.rzg.mpg.de/~mam>



Index

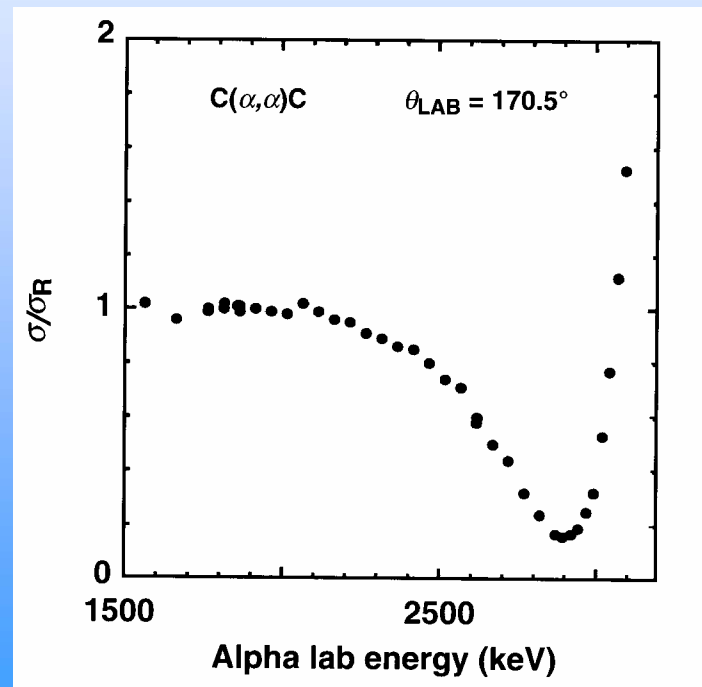
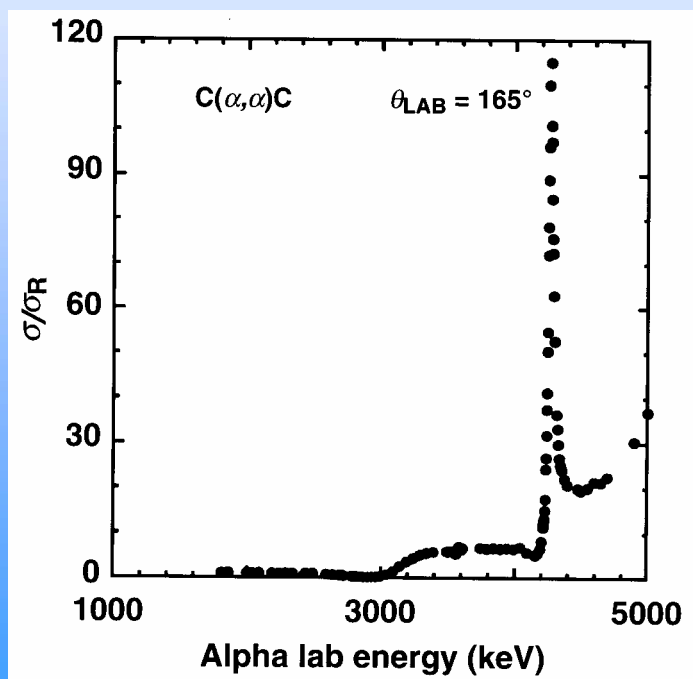
- History
- Scattering geometry and kinematics
- Rutherford cross section and limitations
- RBS spectra from thin and thick films
- Stopping power and energy loss
- Detector resolution
- Energy loss straggling
- Cross sections from selected light elements
 - incident ^1H
 - **incident ^4He**



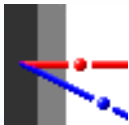
$^{12}\text{C}(\alpha, \alpha)^{12}\text{C}$

IPP

- Small cross section at $E < 3000$ keV
⇒ not suitable for RBS
- High and smooth cross section around 4000 keV
- Maximum sensitivity at 4270 keV



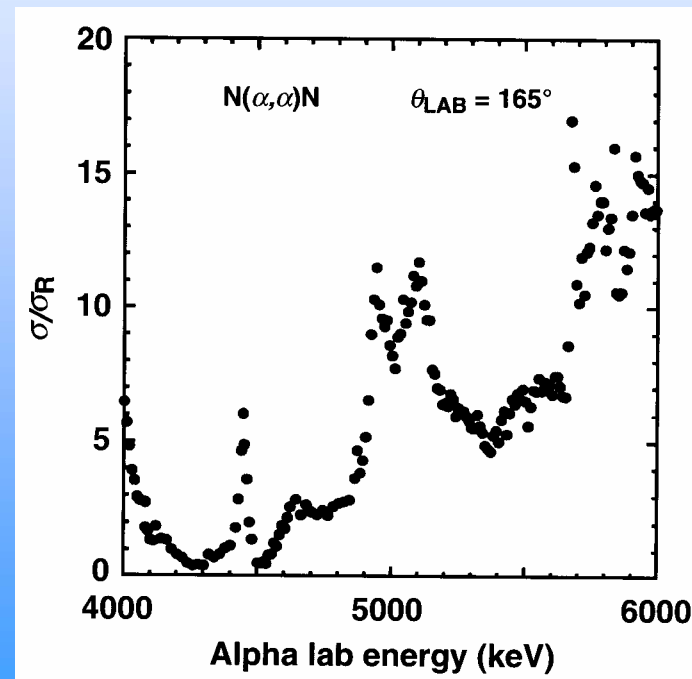
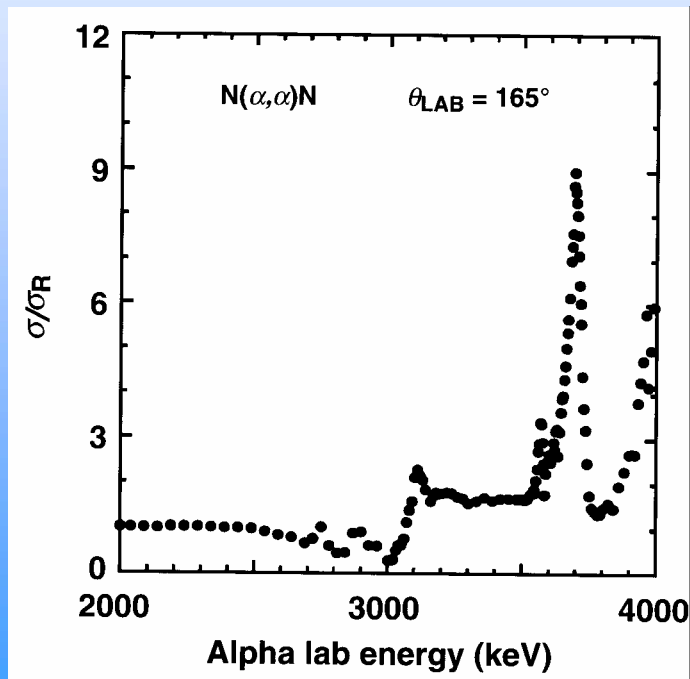
J.R. Tesmer and M. Nastasi, Handbook of Modern Ion Beam Materials Analysis, MRS, 1995



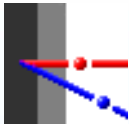
$^{14}\text{N}(\alpha, \alpha)^{14}\text{N}$



- Small cross section at $E < 3000$ keV
⇒ not suitable for RBS
- Several useful resonances at higher energies



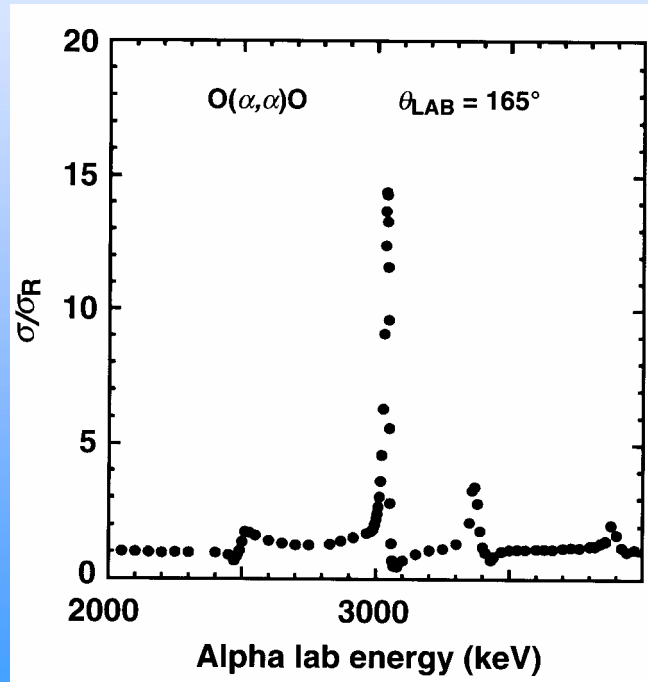
J.R. Tesmer and M. Nastasi, Handbook of Modern Ion Beam Materials Analysis, MRS, 1995



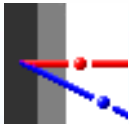
$^{16}\text{O}(\alpha, \alpha)^{16}\text{O}$



- Widely used resonance at 3040 keV

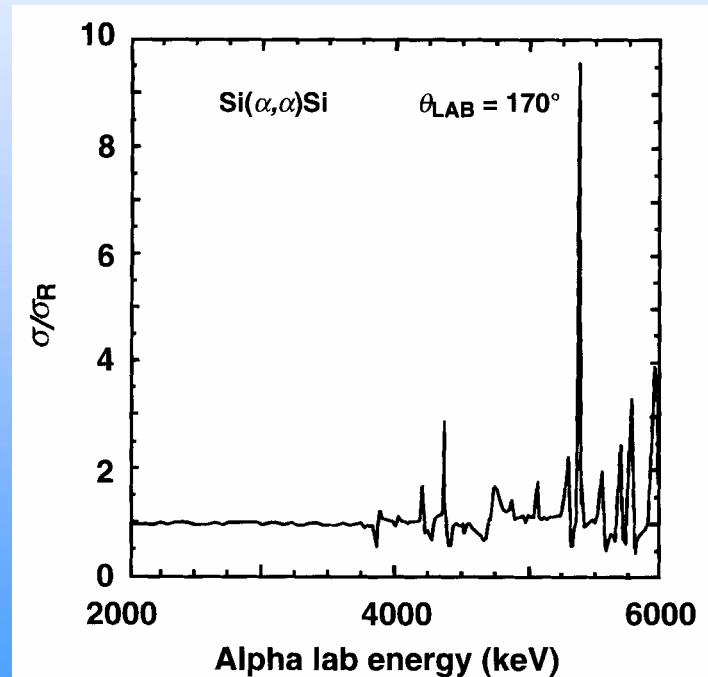
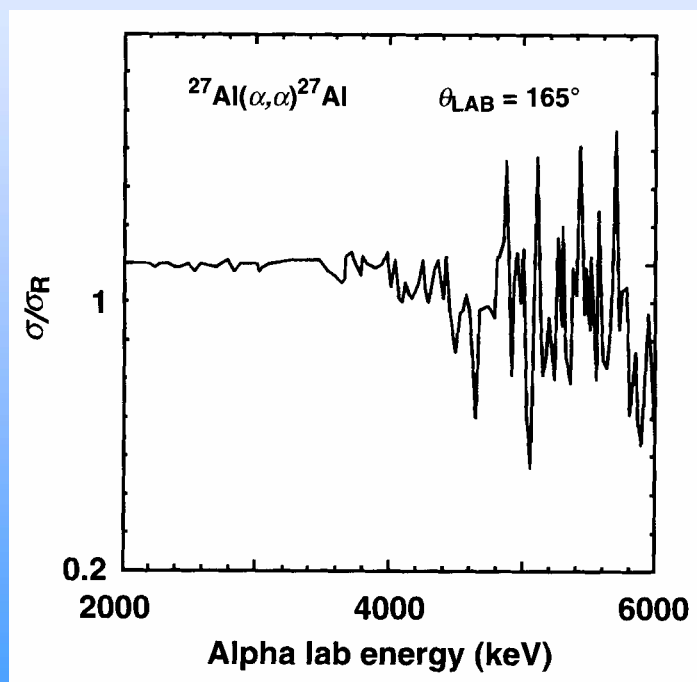


J.R. Tesmer and M. Nastasi, Handbook of Modern Ion Beam Materials Analysis, MRS, 1995

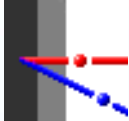


IPP

- Many resonances and small cross sections
⇒ not suitable for RBS



J.R. Tesmer and M. Nastasi, Handbook of Modern Ion Beam Materials Analysis, MRS, 1995



Computer Simulation Codes

IPP

	Program	Author	Since
Spectrum simulator	RUMP	M. Thompson Cornell University USA	1983
	RBX	E. Kótai Research Institute for Particle and Nuclear Physics Hungary	1985
	SIMNRA	M. Mayer Max-Planck-Institute for Plasma Physics Germany	1996
Depth resolution	DEPTH	E. Szilágyi Research Institute for Particle and Nuclear Physics Hungary	1994
Depth profile	WINDF	N. Barradas Technological and Nuclear Institute Sacavem Portugal	1997